

University of Memphis

University of Memphis Digital Commons

---

Electronic Theses and Dissertations

---

8-10-2012

**Layer Parallel Shortening: A Mechanism Used to Determine the Sequence of Deformation of the Little Water Syncline in the Tendoy Mountains, Southwestern Montana.**

Kera Ann Judy

Follow this and additional works at: <https://digitalcommons.memphis.edu/etd>

---

**Recommended Citation**

Judy, Kera Ann, "Layer Parallel Shortening: A Mechanism Used to Determine the Sequence of Deformation of the Little Water Syncline in the Tendoy Mountains, Southwestern Montana." (2012). *Electronic Theses and Dissertations*. 516.

<https://digitalcommons.memphis.edu/etd/516>

This Thesis is brought to you for free and open access by University of Memphis Digital Commons. It has been accepted for inclusion in Electronic Theses and Dissertations by an authorized administrator of University of Memphis Digital Commons. For more information, please contact [khggerty@memphis.edu](mailto:khggerty@memphis.edu).

LAYER PARALLEL SHORTENING: A MECHANISM USED TO DETERMINE THE  
SEQUENCE OF DEFORMATION OF THE LITTLE WATER SYNCLINE IN THE  
TENDOY MOUNTAINS, SOUTHWESTERN MONTANA.

by

Kera A. Judy

A Thesis

Submitted in Partial Fulfillment of the

Requirements for the Degree of

Master of Science

Major: Earth Sciences

The University of Memphis

August 2012

## **Acknowledgements**

I would like to first thank my Mother and Don, for without their unfailing support, this achievement would not have been possible.

I also would like to express my sincere gratitude to my advisor, Dr. Jerry Bartholomew, who has the patience of Gandhi. A finer mentor could not exist for a fledgling geologist like me.

## Abstract

Judy, Kera A., M.S. The University of Memphis. August 2012. Layer Parallel Shortening: a mechanism used to determine the sequence of deformation of the Little Water syncline in the Tendoy Mountains, southwestern Montana. Major Professor: Dr. M.J. Bartholomew.

The Little Water syncline is a complex structural feature within the Tendoy thrust sheet which formed during two temporally overlapping deformational episodes during the Late Cretaceous. The NNW-trending Four Eyes Canyon thrust and the structurally lower Tendoy thrust are associated with NE-SW-shortening related to the Cordilleran (Sevier-style) fold-thrust belt. The Tendoy thrust forms the structural front of the Cordilleran fold-thrust belt in southwestern Montana and its detached, NNW-trending overturned limb (of the Little Water syncline) was over-ridden by the Four Eyes Canyon thrust. Earlier research primarily used stratigraphic evidence coupled with geometric interpretations to suggest that: 1) clasts found in the syn-tectonic (Cretaceous) Beaverhead Formation were derived from the Four Eyes Canyon thrust; 2) Laramide-style deformation occurred before emplacement of the Tendoy thrust sheet; and 3) that the Tendoy thrust was then emplaced over the syn-tectonic Beaverhead Formation. The NE-trending (approximately  $30^{\circ}$ ), overturned northern flank (at nearly right angles to the detached overturned limb) of the Little Water syncline has long been argued to be a structural feature associated with NW-SE-shortening ( $\sim 120^{\circ}$ ) generally related to the Laramide Snowcrest thrust system.

In this study of the Little Water syncline, I have used layer-parallel-shortening (LPS) strain-indicators (fossils and pellets) to obtain the initial direction of shortening preserved in: 1) the NNW-trending, detached, vertical-to-overturned, western limb; 2) the

steeply-dipping-to-overturned, northwestern limb; and 3) the moderately W-dipping, upright, N-trending eastern limb to determine the initial deformation (Sevier or Laramide) that affected the syncline. When bedding is unfolded, LPS strain: at 11 of 14 sites is consistent with NE-SW-shortening ( $221^{\circ}$ ) associated with the Sevier orogeny; at 2 sites is consistent with N-S-shortening; and at 1 site is consistent with E-W-shortening. No sites have LPS strain consistent with NW-SE-shortening. Hence Sevier LPS strain occurred before Laramide deformation. The 3 sites (sites 1, 2, and 5) where LPS strain lies outside of Sevier-shortening ( $221^{\circ} \pm 20^{\circ}$ ), but not within the range of Laramide shortening ( $\sim 110^{\circ}$ - $290^{\circ}$ ) likely represent Sevier LPS strain affected by local factors not accounted for in the retro-deformational sequence used to restore bedding to horizontal in this study.

## TABLE OF CONTENTS

Introduction	1
Previous Work	7
Geologic Setting	11
<i>Timber Butte Anticline and Little Water Syncline</i>	11
<i>Four Eyes Canyon Thrust</i>	12
<i>Tendoy Thrust System</i>	12
<i>Red Rock Fault</i>	13
<i>Muddy Creek Basin Fault</i>	13
Stratigraphy of the Little Water Syncline Area	14
<i>Mississippian</i>	
Mississippian Undivided Formation	14
<i>Pennsylvanian</i>	
Quadrant Formation	16
<i>Permian</i>	
Phosphoria Formation	16
<i>Triassic</i>	
Dinwoody Formation.	17
Woodside Formation	18
Thaynes Formation	18
<i>Jurassic</i>	
Jurassic Undivided Formation	19
<i>Cretaceous</i>	
Kootenai Formation	20
Blackleaf Formation	21
Beaverhead Formation	22
<i>Tertiary</i>	
Muddy Creek Formation	23
Six Mile Formation	23
Methods	24
<i>LPS Strain</i>	24
<i>Data Analysis</i>	24
<i>LPS Samples Collected from the Thaynes Formation</i>	26

Results and Discussion	41
Conclusion	43
References	44

## LIST OF FIGURES

Figure	Page
1. Map of location with major tectonic features	1
2. Map of NE-trending Laramide structures and NNW-striking Sevier thrusts	2
3. Map of significant structures of the Little Water syncline area	3
4. Geologic map of the Dixon Mountain Quadrangle	5
5. Cross-section through the Little Water syncline	6
6. Stratigraphic column of the units present in the research area	15
7. Fry plots generated for this study from data at site 4	28
8. Photograph of a sample containing a high density of peloid fossils	30
9a. Photograph of a sample containing several <i>Pentacrinus</i> sp. fossils	31
9b. Photograph of the same sample with applied strain ellipses	32
10. Stereonets of poles to bedding within the Little Water syncline and Timber Butte anticline	34
11. Stereonets of poles to bedding in the backlimb of the Little Water syncline and in Hidden Pasture Canyon	35
12. Stereonets corrected for local trend and plunge of the Little Water syncline	36
13. Stereonets corrected for local trend and plunge of the Timber Butte anticline and Little Water syncline	37
14. Series of stereonetts illustrating the process for retro-deformation in order to restore the axis of shortening to its original horizontal orientation	38
15. The orientation of all sample shortening axes before and after deformation of bedding	40
16. Sample sites assigned with associated strain ellipses	42



## INTRODUCTION

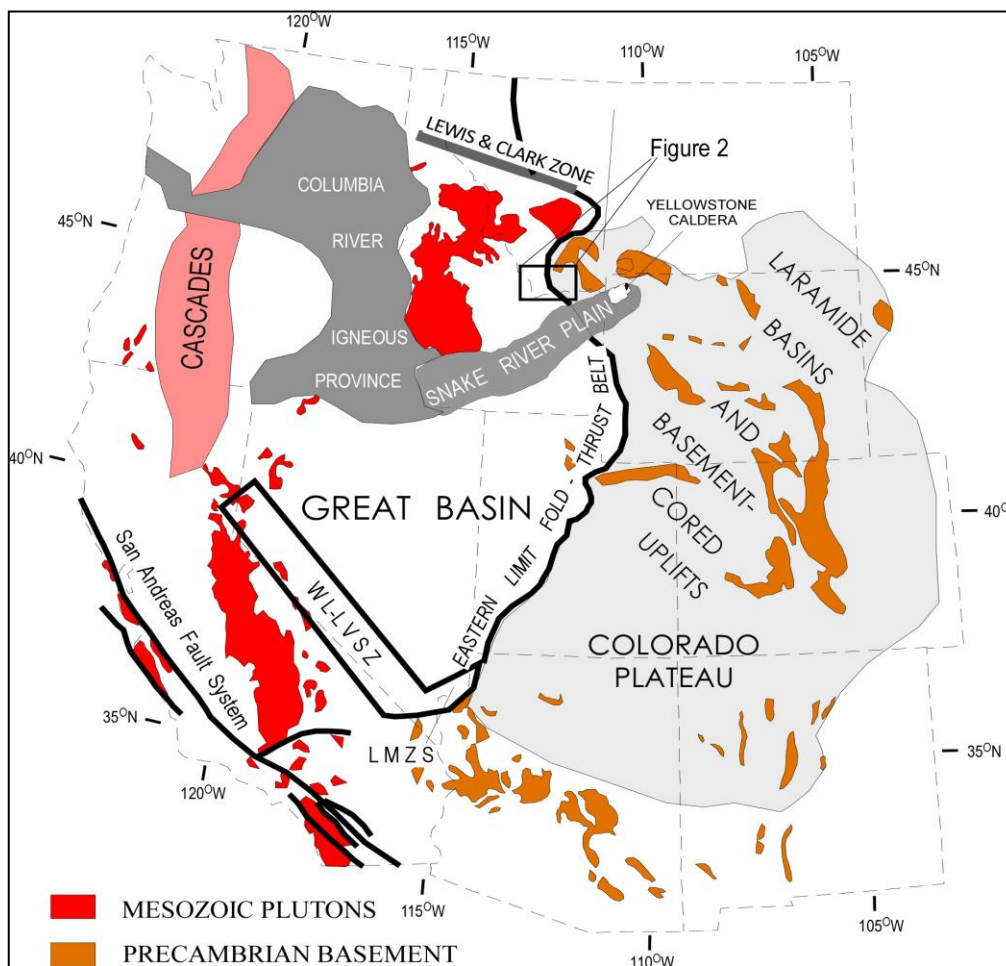


*Figure 1:* Map showing location of study area (Figure 2) relative to Major tectonic features of the Cordillera.

Paleozoic and Mesozoic strata within the Tendoy Range (Figures 1, 2) in southwestern Montana were subjected to two major orogenic events during the Cretaceous. Thin-skinned fold-thrust-belt deformation with E-W-shortening is attributed to the Sevier orogeny (Oldow et al., 1989) which ended during the late Cretaceous. Whereas localized magmatism and thick-skinned basement uplifts (Oldow et al., 1989) are attributed to the Laramide orogeny, which continued into the Tertiary. The Laramide

orogeny affected an area several hundreds of miles in width which lies east of the structural front of the Sevier fold-thrust belt (Figure 1). Laramide structures are characterized by N-S- or NW-SE-shortening.

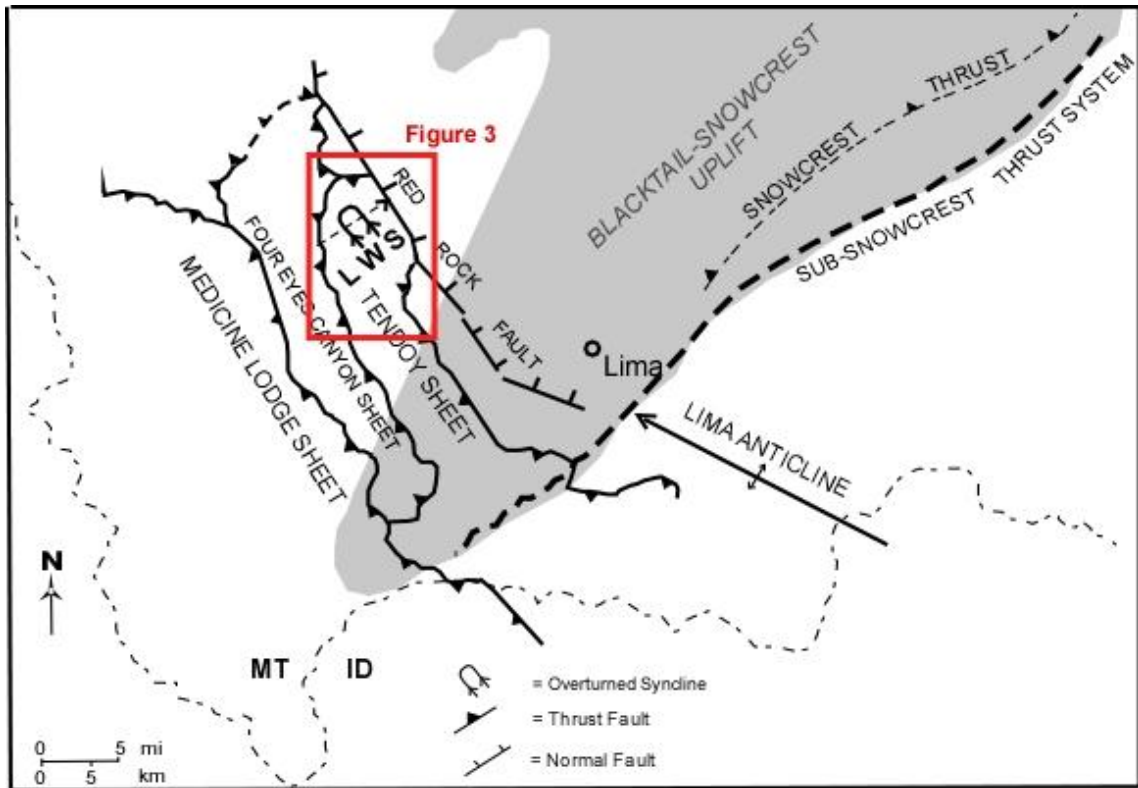


*Figure 2: Map showing NE-trending Laramide structures and NNW-striking thrusts of the Tendoy Range in southwestern Montana, including the Little Water syncline (LWS) (modified after Perry et al, 1988 and Perry et al., 1989).*

In southwestern Montana (Figures 1 and 2), the two events overlapped temporally and spatially during the Late Cretaceous in and near the Tendoy Range where the Tendoy thrust forms the structural front of the Sevier fold-thrust belt (Figure 2). Here, previous authors considered emplacement of the Four Eyes and Tendoy (Sevier) thrust sheets to be coeval with folding of the Little Water syncline (Figure 2 and 3) (Scholten et al, 1955;

Perry and Sando, 1982; Williams, 1984; Perry et al., 1988; Williams and Bartley, 1988; McDowell, 1997), with the syncline interpreted as a complex structure found within the

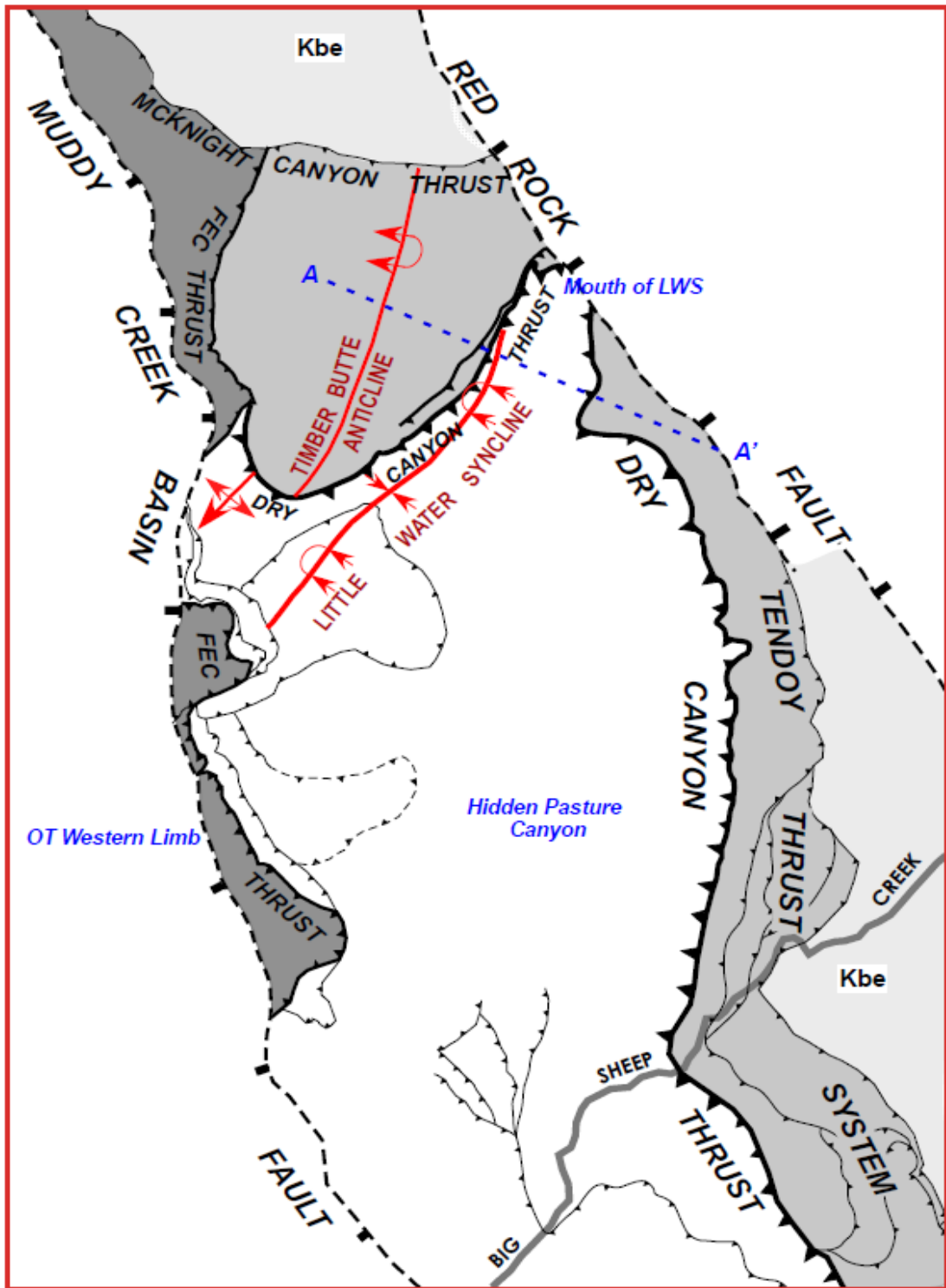


Figure 3: Map illustrating significant structures of the Little Water Syncline area. Line denoted A to A' is the length of cross-section in Figure 4.

Tendoy thrust sheet. Forelandward, near the Tendoy thrust, the axis of the Little Water syncline trends ENE and its northern limb is overturned. Hinterlandward, in the footwall of the Four Eyes Canyon thrust, the detached, overturned limb of the footwall syncline trends N (Bartholomew, 1989a). Thus Bartholomew (1989a) questioned the timing of the folding of two nearly perpendicular overturned limbs of the Little Water syncline relative to thrusting related to the Cordilleran fold-thrust belt and Laramide deformation.

Additionally, he pointed out that the Dry Canyon thrust (generally considered as part of the Tendoy thrust system) climbs up-section, from Mississippian strata near the base of the Tendoy thrust system, northward to a detachment level in the Jurassic mudstones and is folded by the Little Water syncline (Figures 4 and 5). The question addressed in this paper is: did the NE-trending, overturned Little Water syncline and associated Timber Butte anticline form before or after the N-trending, overturned, detached limb of the footwall syncline beneath the Four-Eyes Canyon thrust? Comparison of layer-parallel-shortening (LPS) strain in these nearly perpendicular overturned fold-limbs is a means of discerning which occurred first (e.g. Whitaker & Bartholomew, 1999).

Strain resulting from compression is recorded in many different ways (e.g. folds, faults, cleavage, stylolites) in different types of lithologies. But features such as mudcracks, reduction spots, burrows, oolites and fossils, which lie within or perpendicular to the bedding plane, can provide measurable indications of LPS strain. If protected from subsequent strain by being preserved within a vertical or slightly overturned fold limb, these features can provide critical information of the initial direction of LPS strain (e.g. Whitaker & Bartholomew, 1999). LPS strain, when



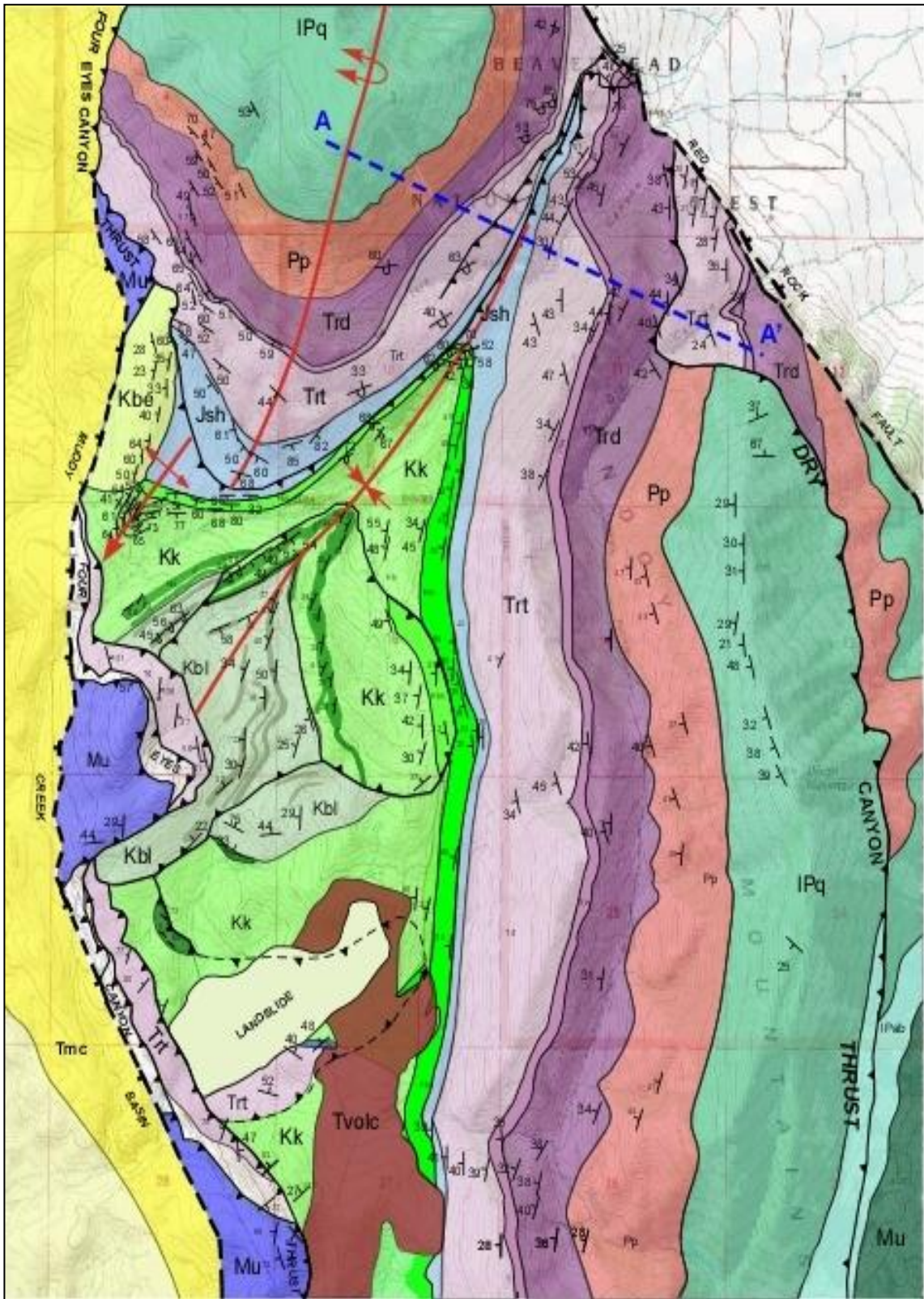


Figure 4: Geologic map of the northern part of the Dixon Mountain Quadrangle. Unit labels are as following: undivided Mississippian strata (Dark Green, Mu), The Quadrant Formation (Sea Green, IPq), The Phosphoria Formation (Coral, Pp), The Dinwoody

Figure 4 (continued): Formation (Purple, Trd), The Woodside Formation (Lavender, Trw), The Thaynes Formation (Light Purple, Trt), undivided Jurassic strata (Light Blue, Jsh), The Kootenai Formation (Pale Lime Green, Kk), Blackleaf Formation (Sage Green, Kbl), The Beaverhead Conglomerate (Yellow-Green, Kbe), Muddy Creek Formation (Golden Yellow, Tmc). Tertiary volcanics and landslides are labeled as Tvolc and Landslide, respectively. Map was compiled from unpublished data from Bartholomew with additional information from Harkins (2002), Klecker (1980), and Dunlap (1982).

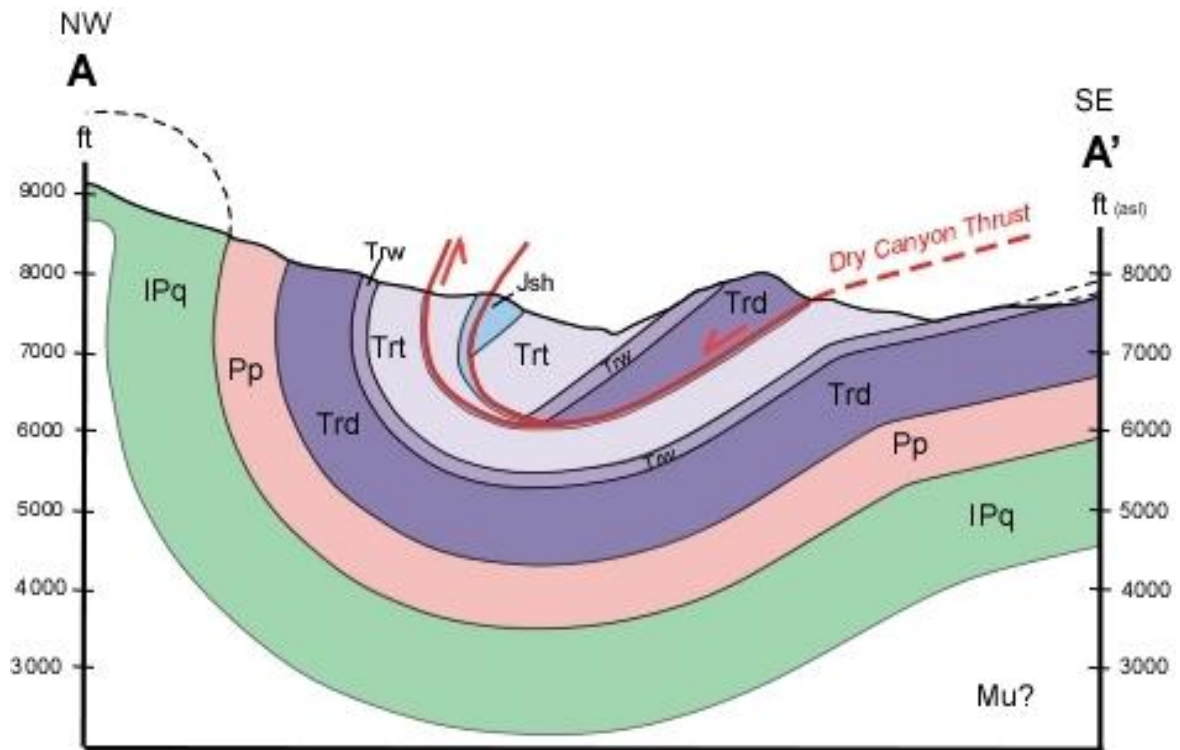


Figure 5: Cross section through the Little Water syncline, showing folding and overturning of the Dry Canyon thrust.

combined with fracture-set data from both overturned and upright fold limbs, can be used to determine the sequence of events in areas where different stress fields overlap in space and time (e.g. Bartholomew & Whitaker, 2010). By analyzing such features, it is possible to determine the initial direction of LPS-strain ( $S_{Hmax}$ ) induced when the beds were horizontal. Thus, if rocks were subjected to two or more differently-oriented stress-fields, LPS-strain can be used to determine which came first (e.g. Whitaker &

Bartholomew, 1999; Bartholomew & Whitaker, 2010). The purpose of this study is to determine the direction of the earliest LPS-strain that affected the Little Water syncline, thus indicating which initiated first: Sevier or Laramide deformation. This was done by using the normalized Fry method (Fry, 1979) to create strain ellipsoids from deformed fossils in samples collected within different limbs of the syncline (Waldron & Wallace, 2007).

### **PREVIOUS WORK**

In the first comprehensive study of the geology of the Lima (Figure 2) region, Scholten et al. (1955) attributed both the NE-trending Snowcrest uplift and the NNW-trending thrusts to the Laramide orogeny. At that time, Cordilleran-style folding and thrusting was not recognized here. This regional study was followed by work on the syn-tectonic Beaverhead Conglomerate (e.g. Ryder & Ames, 1970; Ryder & Scholten, 1973). A decade later, Perry & Sando (1982) focused on determining the sequence of deformation of the Cordilleran thrust belt near Lima based on the timing of syn- and post-orogenic conglomerates. From determination of relative ages of key stratigraphic units, specifically the Cretaceous Beaverhead Conglomerate and facies of the Mississippian Madison Group, combined with cross-cutting relations of the Tendoy and Four Eyes Canyon thrusts, Perry and Sando (1982) concluded that thrusting progressed eastward from the hinterland toward the foreland. Their work is consistent with earlier studies of the Cordilleran fold-thrust belt to the north of this region in Canada (e.g. Dahlstrom, 1969; Bally et al., 1966) and to the south in Utah (Dixon, 1972; Boyer, 1986) which had previously determined that the Cordillera fold-thrust belt developed from the hinterland



toward the foreland (west to east). Perry and Sando (1982) did not mention the Little Water syncline, but indicated the frontal Tendoy thrust was the youngest feature of the Cordilleran fold-thrust belt in the Tendoy Range. Bartholomew (1989b) showed that folds in the basal duplex of the Tendoy thrust system in the Big Sheep Creek area (Figure 3) were oriented consistent with their development during development of the Cordilleran fold-thrust belt deformation.

Perry et al. (1988) first discussed the overlapping structural styles of the Sevier and Laramide orogenic events. They suggested that Laramide deformation began in the Santonian (Late Cretaceous) with growth of the Blacktail-Snowcrest uplift (Figure 2), using superposed syn-orogenic stratigraphic units to date this occurrence. Geological and geophysical data reported in their study showed that the NE-trending Blacktail-Snowcrest uplift and thrust system extended beneath the NNW-striking Cordilleran thrust belt near Lima, and are responsible for the accurate geometry of the Tendoy thrust sheet in this region. According to Perry et al. (1988), formation of the Little Water Syncline occurred during Laramide deformation. Perry et al. (1988) indicated that continued Sevier/Cordilleran deformation then post-dated Laramide deformation after the Snowcrest thrust system was no longer active (~78 Ma), with the NNW-trending imbricate frontal thrusts overriding the NE-trending Snowcrest uplift and thrust system. They concluded that the eastern part of the Little Water Syncline axial trace was rotated counterclockwise due to deformation associated with emplacement of the Sevier-age Tendoy thrust sheet. The syncline was interpreted to be a foreland structure, which was originally a footwall syncline associated with the buried NW-trending Kidd thrust system beneath the McKnight Canyon area. This decapitated footwall structure was

amalgamated to the Tendoy thrust sheet and transported northeastward with it as part of the Cordilleran fold-thrust belt.

Williams and Bartley (1988) examined the stratigraphic and structural relationships in the region containing McKnight and Kelmbeck Canyons which adjoins the study area to the north along the trend of the Cordilleran fold-thrust belt. They attributed most deformation in the Tendoy Range to be Laramide in age, with two different major sets of structural features: the Snowcrest thrust system which includes mainly NE-trending foreland (Laramide) structures; and the Medicine Lodge (e.g. Four Eyes Canyon) and Tendoy thrust systems which comprise thin skinned Cordilleran-type structures that trend NNW. Because this study area is north of the Little Water syncline, no mention of the syncline was made.

Perry et al. (1989) summarized the compressional structural and tectonic elements of the southern part of the southwestern Montana recess and discussed the criteria, commonly stratigraphic, by which these elements were identified. They adhered to their previous estimates (Perry & Sando, 1982; Perry & Hossack, 1984) of the timing of emplacement of the Cordilleran thrusts, attributing the imbricate sheets to Sevier-style deformation.

Many other studies, related to the geology of the area near Lima, have been done and were incorporated in the 1:100,000-scale map (Lonn et al., 2000). This body of work includes numerous additional publications by Scholten (1957, 1967) and Ryder and Scholten (1973) and Harvard University dissertations (Gealy, 1953; Zeigler, 1954) concerning the geology of the Snowcrest Range. Geologic studies of the Tendoy Range include Oregon State University theses (Klecker, 1981; Sadler, 1980) and Texas A & M

structural studies (Hammons 1981; Ponton, 1983). The structure of the northern Tendoy Mountains and adjoining areas to the north and east was done by de la Tour-du-Pin (1983). McDowell (1997) studied the relationships of stratigraphy and structure within the Tendoy thrust sheet to the south of the Little Water syncline. University of Montana theses deal with the Tertiary stratigraphy and structure of the Muddy Creek basin (Dunlap, 1982), the stratigraphy and sedimentology of the Triassic Thaynes Formation (Sikkink, 1984), and neotectonics and gravity modeling of the Red Rock basin (Johnson, 1981a,b). Bartholomew et al. (2009) and Harkins et al. (2005) studied effects of the active Red Rock fault on geomorphic features and the Red Rock basin. Other studies dealing with stratigraphic and structural relations of the Muddy Creek basin were done by Janecke (1994) and Janecke et al. (1999, 2000). Stratigraphic studies include other general reports on localized stratigraphy of the Tendoy thrust and surrounding areas (Moritz, 1951; Sloss & Moritz, 1951; Sandberg & Mapel, 1967; Swanson, 1970; Dyman, 1985a; Dyman et al., 1984; Pecora, 1981; Perry et al., 1983b; Peterson, 1981, 1985; Sandberg et al., 1983, 1985; Sando et al., 1985; Saperstone & Etheridge, 1984; Wardlaw & Pecora, 1985). Studies of Laramide synorogenic sedimentation include those by Lowell & Klepper (1950), Wilson (1967, 1970), Ryder & Scholten (1973) and Haley (1983a, 1983b, 1986). Palynostratigraphic age relations of synorogenic deposits were discussed by Ryder and Ames (1970) and Nichols et al (1985). The sedimentology of the Lower Cretaceous rocks was thoroughly investigated by Dyman (1985b). Structural studies include those by Perry et al, (1981, 1983a, 1985), Perry & Sando (1983), Perry & Hosack (1984), Ruppel & Lopez (1984), Skipp (1988, 2004), Williams (1984), Williams & Bartley (1983), and Bartholomew (1989b).

## GEOLOGIC SETTING

The Tendoy Range is located in Beaverhead County, southwestern Montana. The Little Water syncline, Four Eyes Canyon thrust and Tendoy thrust are located just to the northwest of Lima, which lies at an elevation of ~1890-m, ~128-km west of Yellowstone National Park (Perry et al., 1988) (Figure 1).

Southwestern Montana was subjected to two significant orogenic events: The Sevier Orogeny (140-50 Ma) and the Laramide Orogeny (75-35 Ma) (Dickinson, 1988). These two orogenies are characterized and distinguished by differences in deformational style. The Sevier Orogeny is generally characterized by the roughly N-S to NW-SE-trending, W- to SW-dipping thin-skinned fold-thrust belt, while Laramide structures involve thick-skinned, basement-involved deformation and localized magmatism (Oldow et al., 1989). The large amplitude, NE-striking Little Water syncline is a structural feature associated with NW-SE-shortening generally attributed to the Laramide-style (thick-skin) Snowcrest uplift and thrust (Figure 2), while the NNW-striking Four Eyes Canyon and Tendoy thrusts are structural features associated with NE-SW-shortening related to the Sevier-style (thin-skinned) Cordilleran fold and thrust belt (e.g. Scholten et al., 1955; Williams & Bartley, 1988; Perry et al., 1988; Bartholomew, 1989b) (Fig 2).

### *Timber Butte anticline and Little Water syncline*

The Timber Butte anticline is a NNE-trending, SW-plunging fold with the Quadrant Formation forming its exposed core and creating the topographic relief of Timber Butte (Figures 3 and 4). The southeastern fold limb is overturned. The Little Water syncline is also a NNE-trending, SW-plunging Laramide structure with an overturned northwestern fold limb. Perry & Sando (1988) attribute the overturned fold-

limb of the syncline to the propagation of a Laramide-age sub-surface, NW-dipping blind thrust. Fold axes of both the Timber Butte anticline and the Little Water syncline are deflected southeastward as the folds change northeastward from open, upright folds into overturned folds. The axis of the Timber Butte anticline is decoupled along the Dry Canyon thrust in Jurassic mudstones. Nearby the axis of the Little Water syncline bends to a more northerly-oriented trend (Figures 3 and 4). This might be due to further propagation of the Timber Butte blind thrust, which subsequently tightened both folds, as well as caused a decoupling of the Timber Butte anticline in the weak lithology of the Jurassic mudstones.

#### *Four Eyes Canyon Thrust*

The oldest of the Sevier-generated thrusts in the study area, the Four Eyes Canyon thrust, has a NNW-trend, and is truncated in several locations by the normal fault bounding the Tertiary Muddy Creek basin (Figures 3 and 4). Perry et al. (1988) considered the thrust fault to terminate northward at its intersection with the younger McKnight Canyon thrust.

#### *Tendoy Thrust System*

The Tendoy thrust system consists of a basal duplex structure in the Big Sheep Creek area (Figure 3) with structurally higher thrusts ramping stratigraphically upward to the north (Figures 3 and 4). The basal duplex developed adjacent to the overturned footwall syncline within the Beaverhead Formation in the Big Sheep Creek area (Bartholomew, 1989b). Northward of Big Sheep Creek, where the Tendoy thrust rests on the Beaverhead Formation, the duplex structure is terminated and its roof fault becomes the basal thrust until it is truncated by the Quaternary Red Rock normal fault. The basal

Tendoy thrust may be folded about the Little Water syncline in the same manner as the Dry Canyon thrust (Figures 4 and 5).

#### *Dry Canyon Thrust*

The Dry Canyon thrust is interpreted as part of the Sevier-style Tendoy thrust system and soles downward into the basal Tendoy thrust (Bartholomew, 1989b; McDowell, 1997). However, because it ramps upward to the NNW, from Mississippian strata to Jurassic mudstone (Figures 4, 5, and 6), its primary displacement may actually be part of a reactivated Laramide thrust; alternatively, it may also be a preserved lateral ramp along a Sevier thrust. The Dry Canyon thrust is folded about the Timber Butte anticline and the Little Water syncline (Figures 4 and 5). The ramp terminates upward at its inferred intersection with the Four Eyes Canyon thrust. Decoupling along the folded Dry Canyon thrust allowed the nose of the Timber Butte anticline in the hanging wall to fold independently of the nose in the footwall (Figures 3 and 4).

#### *Muddy Creek Basin Fault*

The Muddy Creek basin trends NNW with the Tertiary strata dipping eastward toward the basin-bounding fault. A system of W-dipping normal faults forms the major basin-bounding fault on the east and three small antithetic normal faults are found on the western side of the basin (Janecke et al., 1999). Geochronologic data from Janecke et al. (1999) indicate that syntectonic basin-fill deposits in the Muddy Creek half-graben range from Middle Eocene to late Eocene in age (46 to <35 Ma), suggesting that the Muddy Creek basin fault was active during this period. Her data show that tectonism was relatively long-lived, spanning at least 10 m.y. (Janecke et al., 1999).

### *Red Rock Fault*

The Late Quaternary, N45°W-trending, Red Rock fault flanks the NE-edge of the Tendoy Range (Figure 2), and lies in the region where tectonic regimes related to northern Basin and Range and Yellowstone hotspot activity overlap in time and space (Bartholomew et al, 2009). Post-Laramide extension and Neogene passage of the Yellowstone hotspot caused reactivation of NW-trending Tertiary normal faults and/or other older Laramide or Precambrian faults and inversion of drainage (Fritz & Sears, 1993; Sears et al., 1995; Sears & Fritz, 1998; Sears, 2007; Bartholomew et al., 2009) of the northern Basin and Range Province in southwestern Montana (Stickney & Bartholomew, 1987).

## **STRATIGRAPHY OF LITTLE WATER SYNCLINE AREA**

### *Mississippian*

#### **Mississippian Undivided Formation**

Previous studies (Harkins et al., 2004; Williams & Bartley, 1988; Perry et al., 1989; Perry & Sando, 1988; McDowell, 1997, 1998) subdivided the Mississippian strata into separate formations based on depositional facies. These include, from youngest to oldest: ~90 m of the Amsden Formation (Light- to dark-gray, brown-weathering, marine, thin-bedded, fossiliferous limestone and calcareous sandstone, with a basal limestone conglomerate); ~300 m of the Conover Ranch Formation (Buff-colored, cross-bedded sandstone, finely interbedded sandstone and siltstones, rhythmically bedded black shales, and some light to dark-gray, thin-bedded, fossiliferous limestone); ~210 m of the Lombard Formation (Light- to dark-gray, thin-bedded, fossiliferous limestones,

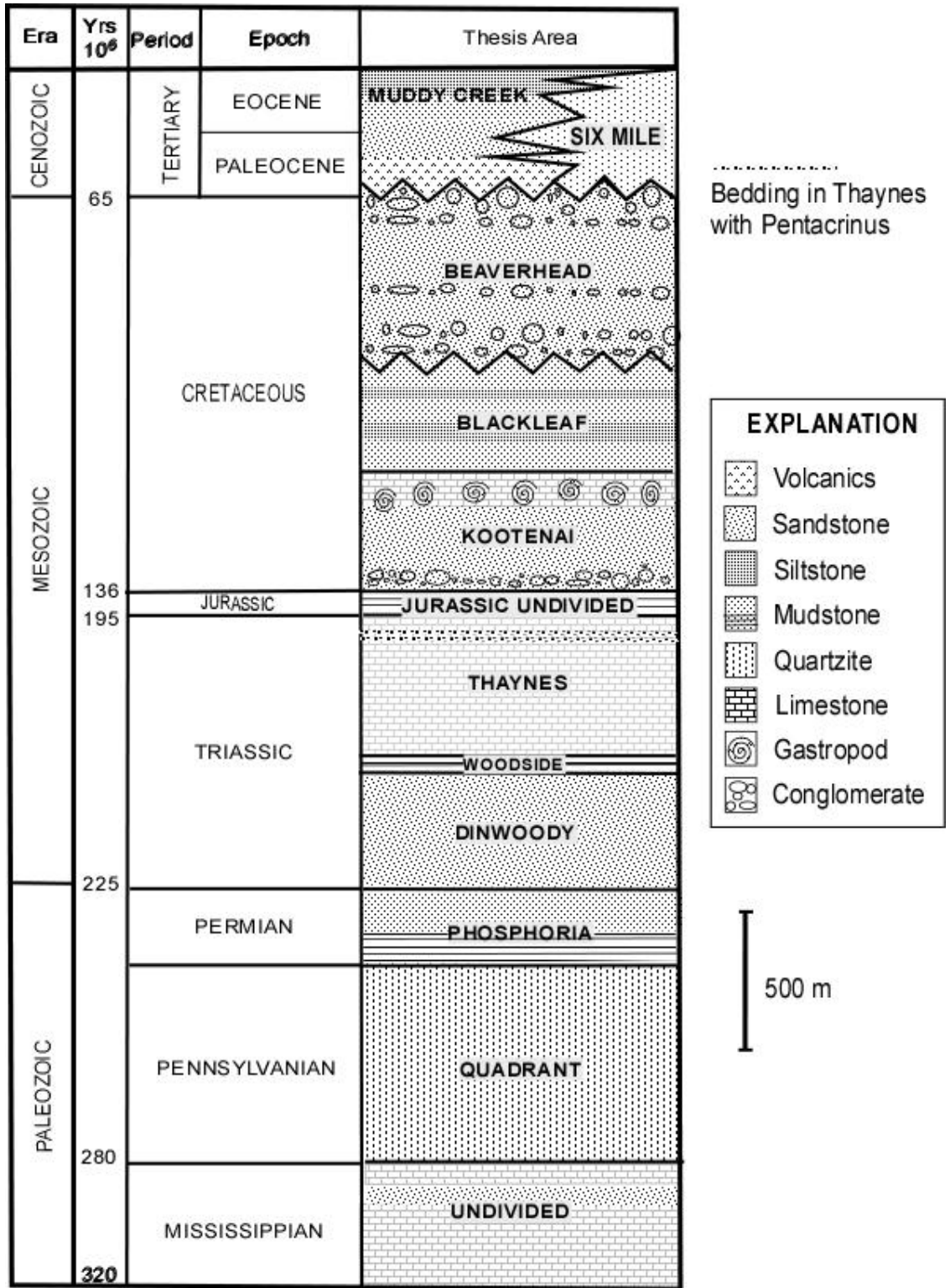


Figure 6: Generalized Stratigraphic column of the units present in research area (modified from Sadler, 1980 and Harkins et al., 2004)



interbedded with buff-colored, calcareous siltstone); ~390 m of the Scott Peak Formation (Light- to medium-gray, thin to massively bedded, cliff-forming, fossiliferous limestone and silty limestone with abundant chert stringers; some portions contain abundant bryozoan and crinoid debris and rudist corals); ~150 m of the Middle Canyon Formation (Medium- to dark-gray, silty limestone and limey mudstone; chert lenses and pods throughout; unit seldom crops out; extensive deformation within this unit prohibits accurate determination of stratigraphic thickness) (Harkins et al., 2004). In this study area, Mississippian strata are sparse, and are grouped as an undivided unit.

### *Pennsylvanian*

#### **Quadrant Formation**

The Quadrant Formation exposures in the Little Water syncline area are generally covered by boulder-size blocky talus that are weathering products of the well-indurated approximately 457 m of sandstone (Perry et al., 1988). The Quadrant is a sandstone/quartzite that is generally thick- to very thick-bedded, planar cross-bedded, with a texture that is variably very fine-grained, and medium-grained, Grey on fresh surfaces, and rust to purple-grey on weathered surfaces. The formation is generally non-fossiliferous (Sadler, 1980; Saperstone et al., 1984, Wardlaw & Pecora, 1985; Saperstone, 1986).

### *Permian*

#### **Phosphoria Formation**

The Phosphoria Formation consists of two members: a lower phosphatic mudstone member about 61 m thick, and the overlying Rex Chert member consisting of about 46 m of bedded chert. This lower member is then overlain by 31 m of mudstone

and cherty mudstone (Sadler, 1980). McKelvey et al. (1956, p. 2845, 2849) named the lower mudstone the Meade Peak Phosphatic Shale Member, and named the upper mudstones the Rex Chert and the Cherty Shale Member. The Meade Peak and Rex Chert names were extended to include beds in western Wyoming and southwestern Montana (Sadler, 1980).

### *Triassic*

The Triassic System of southwestern Montana consists of more than 610 m of three conformable formations (Perry et al., 1988). They are, in ascending order, the Dinwoody, Woodside, and Thaynes Formations. The Dinwoody Formation unconformably overlies the Permian Phosphoria Formation, and the top of the Thaynes Formation is an unconformity spanning Middle Triassic to Early Jurassic (Sadler, 1980).

### **Dinwoody Formation**

In the Little Water syncline area the Dinwoody Formation is ~256 m thick and is divisible into a lower fissile calcareous siltstone member and an upper siltstone-limestone member. The lower member is ~30 m thick and consists of laminated and very thin-bedded calcareous siltstone with isolated interbeds of thinly bedded silty limestone (Sadler, 1980, Scholten et al., 1955). The calcareous siltstones are nonresistant, weathering to shards that are dark yellowish brown and grayish orange on broken surfaces, and weather pale to yellowish brown. Except for stratigraphic position, it is indistinguishable from the silty limestones in the upper member of the Dinwoody. The upper member of the Dinwoody Formation consists of approximately 226 m of interbedded calcareous siltstones and limestones in nearly equal proportions and, to a lesser extent, interbeds of silty limestone (Sadler, 1980). The Dinwoody Formation in the

Little Water syncline area is fossiliferous; however, the fossils are generally very fragmentary or occur only as impressions on bedding planes of the calcareous siltstone (Sadler, 1980).

### **Woodside Formation**

The Woodside Formation in the Little Water syncline is generally poorly exposed, but is interpreted as entirely conformable with the underlying Dinwoody Formation, and the overlying Thaynes Formation (Sadler, 1980; Scholten et al., 1955). The Woodside Formation is 40-m thick, and is made up mostly of fissile, very thinly-bedded and laminated siltstones; minor very fine-grained sandstone can also be identified, interbedded with thin beds of limestone, silty limestone, and dolomite. A noticeable feature of the fossiliferous Woodside is the red splash of color formed by the weathered siltstones. Colors of freshly exposed siltstone are quite variable (Sadler, 1980; this study).

### **Thaynes Formation**

In the Dixon Mountain area, the Thaynes consists of 363 m of limestone, calcareous and siliceous sandstone, and mudstone. These three subdivisions, described by Moritz (1951), were also recognized by Scholten et al. (1955, p. 366) and Klecker (1980, p. 97). In the Little Water syncline, the limestone in the upper part of the Thaynes Formation is a sparse to packed biosparite that is usually a very pale tan, to a yellowish brown. Etched out in high relief on weathered surfaces of select limestone bedding in this portion of the Thaynes Formation are circular crinoid columns, *Pentacrinus* sp., pelecypod shell fragments, echinoid plates and spines, and peloids (Scholten et al, 1955, this study). Specific bedding surfaces containing the abundant crinoid, *Pentacrinus* sp. and peloid fossils used in this study for LPS-strain analysis typically range from ~1-1.6-

m in thickness. Nodular chert and discontinuous beds of chert up to 4-cm thick are found in limestone of the middle and upper parts of the formation. The lower limestone member is a packed biomicrosparite with varying mixtures of intraclasts. The limestone here is pale grayish-brown or pale gray on fresh surfaces, and weathers to dark grayish-brown and yellowish-gray (Sadler, 1980; this study).

### *Jurassic*

#### **Undivided Jurassic Unit**

The Undivided Jurassic unit consists of two main lithologies. According to Scholten et al. (1955), the stratigraphically lower unit, the Sawtooth Formation, is restricted to the central and southern part of the Tendoy Range. The formation is 34-m thick in Little Water syncline area, and is made up of two distinct lithologies (Moritz, 1979). The basal layer consists of 18-21-m of gray and gray-green calcareous mudstones which weather into splintery, pencil-shaped fragments and very pale orange to grayish-orange and yellowish gray to dusky yellow thinly laminated to very thinly bedded, micritic limestone. This lower unit weathers to acicular shards and contains rare pelecypod shell fragments (Sadler, 1980). The upper layer is a yellow brown argillaceous limestone, 21-24-m thick, which weathers into small blocky fragments. The upper unit is pale yellowish brown when fresh and weathers to pinkish-gray blocky centimeter-size fragments. Disseminated throughout the rock are clusters and stringers of fine sand-sized pyrite spherulites (Sadler, 1980). In the Little Water syncline area, the mudstone portion of this unit contributes to intense deformation in the overturned limb of the syncline and is the décollement for the Dry Canyon thrust along which the Timber Butte anticlinal fold axis is decoupled.

Moritz (1951, p. 1809-1810) described 33-m of the stratigraphically upper unit of the undivided Jurassic, the Rierdon Formation, in Little Water syncline and 32-m in the Middle Fork of Little Sheep Creek southeast of the thesis area. He noted that the basal unit of the formation in southwestern Montana is a prominently oolitic limestone which is overlain by argillaceous limestone. The argillaceous limestone is very pale orange and yellowish gray and weathers to platy and blocky shards that exhibit signs of deformation; slickensides and fibers as well as fractures and vein fill are common. The oolitic limestone is not restricted to the base of the formation but occurs as discontinuous lenses within the fissile argillaceous micrite (Sadler, 1980).

### *Cretaceous*

#### **Kootenai Formation**

The Kootenai Formation disconformably overlies the undivided Jurassic unit. Where the Morrison is absent, the Kootenai rests unconformably on pre-Jurassic rocks near Lima, Montana and is overlain by the Blackleaf Formation east of a roughly N-S-trending line which passes through Butte, Montana (Moritz, 1951, figure 18). In southwestern Montana the Kootenai is conformably overlain by strata equivalent to the Aspen Formation of Scholten et al. (1955, p. 368). Where pre-Tertiary erosion removed the Aspen Formation, the Beaverhead Formation rests with an angular unconformity on the Kootenai (Perry et al., 1988).

Gwinn (1965, p. 36-37) divided the Kootenai Formation into four mapable members. These are informally called the lower clastic member, the lower calcareous member, the upper clastic member, and the upper calcareous member. The lower clastic member is a regionally recognized basal chert-pebble conglomerate or the salt-and-

pepper medium- to coarse-grained sandstone. The lower calcareous member consists of dark gray and various colored siltstones and mudstones ranging in thickness from 0.3 to 7 m. The upper clastic member ranges in thickness from 122 to 153 m and consists of variegated mudstones and siltstones. The upper calcareous member, better known as the gastropod limestone, is a ledge-forming gray biomicritic limestone attaining a maximum thickness of 71 m west of Drummond, Montana.

Within the Little Water syncline, the Kootenai consists of basal chert-pebble conglomerate overlain by interbedded salt-and-pepper sandstones and reddish siltstones overlain by similar rocks but containing one or, locally, two gastropod limestone beds. The gastropod limestone is a convenient marker for the top of the Kootenai Formation.

### **Blackleaf Formation**

Laying conformably above the Kootenai Formation in the core of the Little Water syncline is approximately 200 m of variegated mudstones with discontinuous beds of sandstone, and siltstone which Sadler (1984) called Colorado Shale. Exposures are poor and lithologic similarities with formations in Wyoming, Idaho, and elsewhere in southwestern Montana make applying a name to this unit difficult (Sadler, 1980). Gwinn (1965) described a Colorado "Group" in the Clark Fork Valley of west-central Montana. He subdivided the Colorado Group into the Blackleaf Formation of Early Cretaceous age and the Coberly, Jeus, and Carter Creek Formations of the Late Cretaceous. Other authors working in the Little Water syncline have also discussed the Kootenai and Blackleaf as the two main units of the Lower Cretaceous (Perry et al., 1988; Perry et al., 1989). Dyman et al. (1994) and Tysdal et al. (1994) provided a more recent description and correlation of the Cretaceous Blackleaf Formation in southwestern Montana. During that

compilation T.S. Dyman visited the Little Water syncline with M.J. Bartholomew and identified these strata in the syncline as Lower Blackleaf Formation.

The thickness of the formation is unknown because of pre-Tertiary erosion prior to deposition of the Beaverhead Formation and Cenozoic erosion which has stripped-off all overlying strata in the Little Water syncline. The formation is made up mostly of non-resistant mudstones, and is generally covered. Sadler (1984) collected samples from a stream bank in the Little Sheep Creek area about 16 km southeast of the thesis area, and documented bluish -gray and greenish-gray calcareous non-fissile silty claystone. Resistant outcrops of laterally discontinuous limestones, sandstones, and siltstones occur from place to place throughout the formation (Sadler, 1980).

### **Beaverhead Formation**

The Beaverhead Formation, previously called the Beaverhead Group (Wilson, 1967; Sadler, 1980; Williams, 1984; Nichols et al., 1985; Perry et al., 1988; Williams & Bartley, 1988) contains two depositional suites: the Lima conglomerate derived from the Blacktail-Snowcrest uplift, and overlying conglomerates and sandstones chiefly derived from the Cordilleran thrust belt (Perry et al., 1988), namely the McKenzie thrust (Williams & Bartley, 1988). The unit ranges from about 250 to 1,000-1,300 m thick, thickening eastward (Lonn et al, 2000). The Beaverhead rocks overlie tightly folded and overturned rocks of older formations with a profound angular unconformity (Lonn et al., 2000). The Beaverhead Formation can be found in the northwestern limb of the Timber Butte anticline where bedding has similar orientations to bedding in the subjacent undivided Jurassic near the plunging apex of the fold hinge. This suggests that both the

Beaverhead Formation and undivided Jurassic unit were subjected to the same compressional regime.

*Tertiary*

### **Muddy Creek Formation**

Basin-fill deposits in the Muddy Creek half graben (Figure 4) include five mappable facies with a cumulative thickness of ~4-km (Janecke et al., 1999). Upward from the basal part of the basin, these units are: Tertiary volcanics, interbedded conglomerate, a tuffaceous shale facies, an organic-rich facies, and a conglomerate and sandstone facies (Janecke et al., 1999). In the study area, these beds are exposed to the west of the Four Eyes Canyon thrust and the basin-bounding Muddy Creek fault.

### **Sixmile Formation**

The Sixmile Formation is equivalent to the Muddy Creek Formation, and is not found in the research area. It is comprised of sandstone, siltstone, and conglomerate units. The sandstone and siltstone unit contains – Light gray and olive-gray to yellowish-gray, pale brownish-gray tuffaceous sandstone and siltstone, with beds ranging from 3.5 to 23 m (10 to 70 ft) thick. Many beds contain isolated small well rounded pebbles of basalt, quartzitic sandstone, and chert. The conglomerate units are characterized by beds 3 to 6 m (10 to 20 ft) thick containing well rounded cobbles and pebbles, mainly of locally derived quartzitic sandstone, chert, limestone, and dolomite, a small percentage of Belt Supergroup pebbles and cobbles derived from the Gravelly Range gravel, and rare boulders of vesicular basalt, as much as one foot in diameter, floating in a pebble-sand matrix (Lonn et al., 2000). Thickness of the formation is estimated to range up to 800-m



thick in the Jefferson Basin near Whitehall, Montana (Keunzi & Fields, 1971); however, this unit has not been mapped in the Little Water syncline area.

## **METHODS**

### *Layer-Parallel-Shortening Strain*

Layer-parallel-shortening (LPS) strain is incipient homogenous strain which occurs within a layered rock when the direction of shortening lies within the plane of the bedding surface, and the layer shortens in a horizontal plane and thickens in a vertical plane as a result (Ramsay & Huber, 1986). LPS strain occurs prior to other forms of strain accommodation, and this first incidence of compression may be well preserved in vertical or overturned limbs, despite subsequent multi-scale deformation (Simon & Gray, 1982; Whitaker and Bartholomew, 1999; Bartholomew and Whitaker, 2010). LPS strain is accommodated at grain-size scales, by intragranular processes such as cataclasis, microfracturing and dislocation flow, and transgranular processes such as compaction and pressure solution. Pressure solution results in stylolites, sutured grain boundaries, and crystal growth (Onasch & Dunne, 1992; Spraggins & Dunne, 2001). Transgranular accommodation is of interest in this study, because these processes result in an alteration of original center-to-center distances of engrained objects.

### *Data Analysis*

Strain analysis is a method of quantifying strain magnitude and/or orientation of principal strain directions. Strain-measurement techniques require measurement of strain indicators to obtain principle strain-axes orientations and axial ratios. The Fry Method (Fry, 1979) of strain analysis utilizes the center-to-center method, in that it requires distances between grain centers (strain indicators) in order to measure strain. The Fry

Method is a graphical approach that uses the distribution of the centers of initially randomly distributed spherical strain indicators to define a strain ellipse for the sample rock in question (Fry, 1979; Ramsay & Huber, 1983). A Fry plot is created by plotting the location of strain-marker centers as a function of distance from every other strain-marker center within the bedding plane of the immediately adjacent rock (Fig 7). This can be done manually by plotting each grain center on a piece of tracing paper overlying a photograph of strain indicators; as the overlay is moved incrementally from center to center of each grain, the shape of the strain ellipse will coalesce from the amalgamation of these plotted strain indicators in the form of a central vacancy field, an elliptical shape in which few or no centers have been plotted. This central vacancy ellipse defines the samples strain ellipse, from which an axial ratio ( $R_s$ ) is calculated. The Fry method is most effective in samples with strongly anti-clustered, initially spherical strain indicators of equal size that are strained homogeneously (Fry, 1979; Crespi, 1986; Dunne et al., 1990; Ramsay & Huber, 1987); the simultaneous occurrence of these qualities is not common in nature. Erslev (1988) sought to compensate for this issue by creating the normalized Fry method. The normalized Fry method accounts for discrepancies in sizes and sphericity of strain indicators, which produces Fry plots with greater definition of the central vacancy field.

Limitations of this simple tool must be considered when employing the Fry method for LPS-strain analysis. Fry strain analyses are inherently labor intensive due to the large size of data sets required to generate an accurate central vacancy field. The normalized Fry method is only valid on rocks that were deformed plastically and will yield inaccurate results if strain is heterogeneous. Strain accumulation through micro-

faulting and sub-grain creation and grain-boundary sliding destroy original strain markers and invalidate assumptions of its initial shape (Dunne et al., 1990). Hence, samples used for analysis must be as close to homogenous in composition as possible, with little-to-no evidence of brittle deformation. The Fry method can be successfully applied only if the distribution of particles is isotropic and anti-clustered. As proposed by Fry (1979) and confirmed by Crespi (1986), the more a population deviates from this type of distribution and tends to be random (Poisson), the less confidence can be placed in the result. Since clustering of centers decrease the ellipse definition on the Fry diagram (Crespi, 1986; Erslev, 1988), a systematic control of the point distribution should be done for unpacked as well as for packed aggregates to have more confidence in the significance of the resulting vacancy field in the Fry diagram (Genier & Epard, 2006). The Fry method is still viable where there is non-uniform (Poisson) grain distribution, if the sample contains >200 randomly distributed strain indicators (Fry, 1979).

#### *LPS Samples Collected from the Thaynes Formation*

The Thaynes Formation is a thinly bedded, yellow-tan to medium-grey, sandy, fossiliferous limestone composed of medium-grained, intergrown crystals (Majerowicz et al., 2007). This unit is suitable for Fry analysis due to the presence of interbedded layers containing mostly uniformly distributed and anti-clustered *Pentacrinus* sp. and peloid fossils (Figures 8 and 9), with a lack of obvious signs of intense deformation (slickensides/fibers, stylolites, joints and fractures).

Fourteen samples from the Thaynes Formation were collected at exposures throughout the Dixon Mountain Quadrangle area. Samples collected were in the form of high-resolution photographs taken perpendicular to the exposed bedding surface.

Photographs were taken at exposures containing bedding surfaces which were replete with strain indicators, i.e. the *Pentacrinus* sp. (stems oriented normal/perpendicular to bedding) and peloid fossils. Data recorded at each sample site include which quadrangle the sample was taken in, the structural location of the sample (with sample number), GPS measurements to ensure accuracy of sample location, attitude (right-hand rule), unit of collected sample, orientation of bedding (right-side-up or overturned) (Table 1), and photographed bedding surfaces were marked with field orientations (close-ups of photographs may not contain these markings). Photographs of each sample were then digitized using ArcMap software. Once uploaded into ArcMap, each photograph was designated a separate layer file. A point-shape file corresponding to each photograph was then added to each layer file in order to highlight the centers of each strain marker, and the point data were subsequently stored in a database file. Each photograph was carefully examined for strain indicators, and the center of each located precisely and marked using a circular symbol. The number of selected strain indicators was targeted at ~250 objects per photographed area to create statistically valid Fry plots. The photographed strain indicators were then analyzed by hand-plotting Fry diagrams using the center-to-center distances of selected strain indicators. Seven of the fourteen samples were found to exhibit satisfactory central vacancy fields, and the ellipse designated to each of these Fry plots was then fitted with both measured long ( $S_1$ ) and short ( $S_2$ ) axes. From these, the axial ratio ( $R_s$ ) was accordingly calculated, and from this ratio, the amount of shortening was ascertained (Figure 7; Table 1).

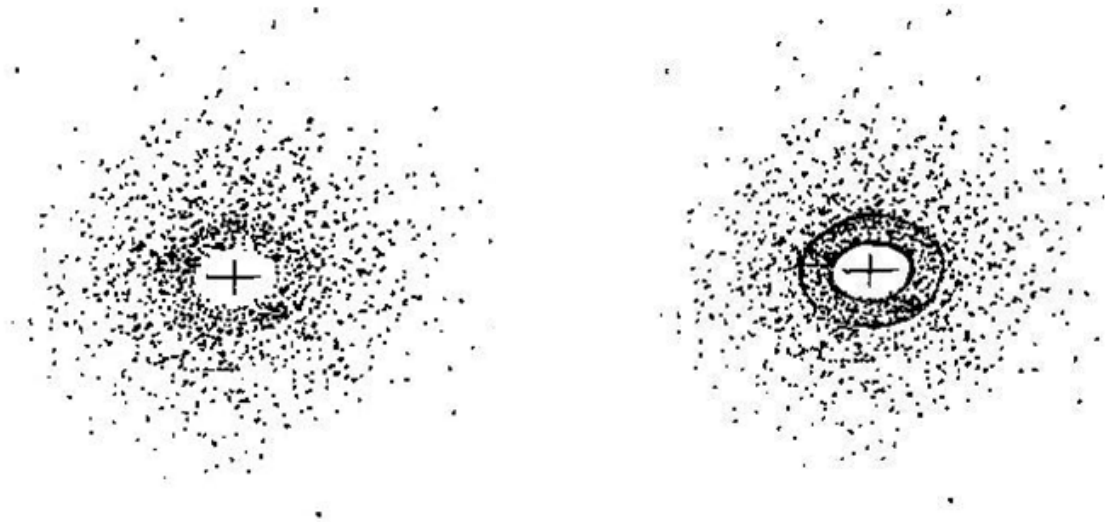


*Figure 7:* Fry plots generated for this study, sample site LWS-PC-4a. Left: nearest-neighbor (Fry) method creates a central vacancy field. Right: central vacancy field and highest point-density ellipses fit to Fry plot.

Table 1: Data collected for all fourteen samples used in this study

SN#	STRUC	STI	PIC#	GPSNUM	GPS1	GPS2	STRIKE	DIP	U	OR/R	Rs	%SH
2	MC	PEL	3b	13	12T0355368	4948875	185	62NW	Trt	R	1.14	13
3	MC	PEL	5b	12	12T0355418	4949357	210	84NW	Trt	R	1.09	9
1	LWS	PEL	1d	16	12T0358425	4954862	210	30NW	Trt	OT	1.07	7
4	MC	PEL	6a	17	12T0355245	4949756	215	70NW	Trt	OT	1.22	19
5	MC	PEL	7b	18	12T0355462	4949368	25	70SE	Trt	OT	1.19	16
6	HP	PEL	1c	19	12T0357701	4948753	190	44NW	Trt	R	1.26	21
7	HP	PC	a*	20	12T0357529	4948750	195	30NW	Trt	R	1.21	18
9	LWS	PC	1b	21	12T0356198	4952767	140	60SW	Trt	R	1.39	29
10	LWS	PC	1c	21	12T0356198	4952767	140	60SW	Trt	R	1.25	20
11	LWS	PC	2c	22	12T0356214	4952775	124	61SW	Trt	R	1.31	24
12	LWS	PC	2c*	22	12T0356214	4952775	124	61SW	Trt	R	1.4	29
13	LWS	PC	3d	23	12T0356229	4952783	121	62SW	Trt	R	1.36	27
14	LWS	PC	4a	24	12T0356253	4952793	126	65SW	Trt	R	1.33	25
8	LWS	PC	4a*	24	12T0356253	4952793	126	65SW	Trt	R	1.31	24

**SN:** Sample number site, with designated strain ellipse, numbers correspond with ellipse numbers on Figure 16.

**ST:** Structure in the Dixon Mountain Quadrangle from which samples were used. **MC:** Muddy Creek basin; **HP:** Hidden Pasture Canyon; **LWS:** Little Water syncline.

**STI:** Strain Indicator in each sample. PEL: pellets; PC: *Pentacrinus*.

**PIC:** Photograph used each photograph taken per sample site. Asterisks (\*) denotes strain ellipse was generated using the hand-fit to *Pentacrinus* method.

**NUM, GPS1 and GPS2:** Precise GPS location of each listed sample.

**STRIKE, DIP:** Attitude of bedding on which each strain ellipse was superimposed. Current day orientation.

**U:** Unit containing sample; all were Thaynes in this study.

**O/U:** Orientation of bedding, O-overturned or U-upright

**Rs:** Ratio of long axis ( $S_1$ ) to short axis ( $S_2$ ) of each samples' generated strain ellipse.

**%SH:** Percent shortening, ascertained by analyzing Rs from a normalized spherical circumference

The magnitude of the shortening was calculated assuming constant volume deformation (i.e. non-solution mechanisms, transgranular interaction like grain-boundary-suturing and compaction). In addition to the strain ellipses generated using the Fry Method (Fry, 1979), photographs containing adequate numbers of deformed *Pentacrinus* sp. fossils were subjected to further strain analysis; this analysis was conducted by observing each individually deformed fossil in the sample/photograph, and thusly encircling each with a properly fitted strain ellipse (Figure 9, bottom). Amount of shortening were determined using this method as well. Any amount of shortening discrepancies between the Fry Method (Fry, 1979) and hand-fit ellipses were found to be insignificant.

To uncover the direction of initial LPS strain, several steps were taken. First, bedding attitudes of the Thaynes Formation exposures throughout the syncline were compiled, plotted, and fitted with an average great circle and pole determination using R.W. Allmendinger's STEREONET v. 4.9.6 for seven different significant locations in the Dixon Mountain Quadrangle. Bedding attitudes collected near the mouth of the Little Water syncline compiled with bedding in the Kootenai Formation of the Little Water syncline provided the trend and plunge of the synclinal fold axis (Figure 10). Attitudes of bedding in the northwestern part of the research area within the Thaynes and Dinwoody Formations paired with attitudes of bedding in the undivided Jurassic unit and in the Beaverhead Formation provided the trend and plunge of the fold axis of the Timber Butte anticline (Fig 10). Attitudes from overturned, detached and upright bedding of the Thaynes Formation in the southwestern limb in and the Thaynes Formation of Hidden Pasture Canyon provided an orientation of these broadly folded bedding surfaces (Figure 11). These data were then restored to horizontal using rotations about the average attitude



*Figure 8:* Photograph collected due to high density of peloid fossils. Sample site MC-PEL-3b.





Figure 9a: Photograph taken due to high concentration of peloid and *Pentacrinus* sp. fossils. Sample site LWS-PC-4a.



*Figure 9b:* Same sample after being analyzed for *Pentacrinus* strain. Strain ellipses are fit to individually deformed fossils, providing orientation and amount of deformation.

of bedding planes of sample sites, (Table 2) and corrected for the local trend and plunge of segments of the Little Water syncline and Timber Butte anticline (Figures 12 and 13).

After retro-deformation of all sample bedding surfaces containing samples providing strain ellipses to horizontal, the data for 7 sites yields a dominant shortening direction of  $221^{\circ}$  (Figure 15, right). However, Bartholomew (1989b) demonstrated in the Big Sheep Creek area (Figure 3) that both bedding and folds were passively folded over a NE-trending lateral ramp. On the down-folded north side of the ramp W-dipping beds strike N-S and fold axes with W-dipping axial surfaces trend N. LPS sites 6 and 7 (Figure 16) are on this north side of the ramp. To the south of the ramp, SW-dipping beds strike NW-SE and fold axes with SW-dipping axial surfaces trend NW. These orientations are consistent with typical Sevier deformation. Because of this apparent vertical rotation that occurs north of the ramp, the affected 6 sites (2-7) are further retro-deformed and rotated 36 degrees counter-clockwise to accommodate for the effects of the lateral ramp (Bartholomew, 1989b) and to align this N-trending section to be consistent with the NW-trending section of the Tendoy thrust before its passage over the lateral ramp.

Because sample photographs were taken perpendicular to bedding surfaces, the orientation of the short axis of the strain ellipse could be plotted as a rake on a bedding plane using STERONET. These rakes and bedding planes were then retro-deformed using the same rotations as were employed in the restoring of fold axes and bedding surfaces to horizontal (Figure 14). These retro-deformed rakes were then used to ascertain the unfolded orientation of  $S_2$  which is the initial direction of the LPS strain.



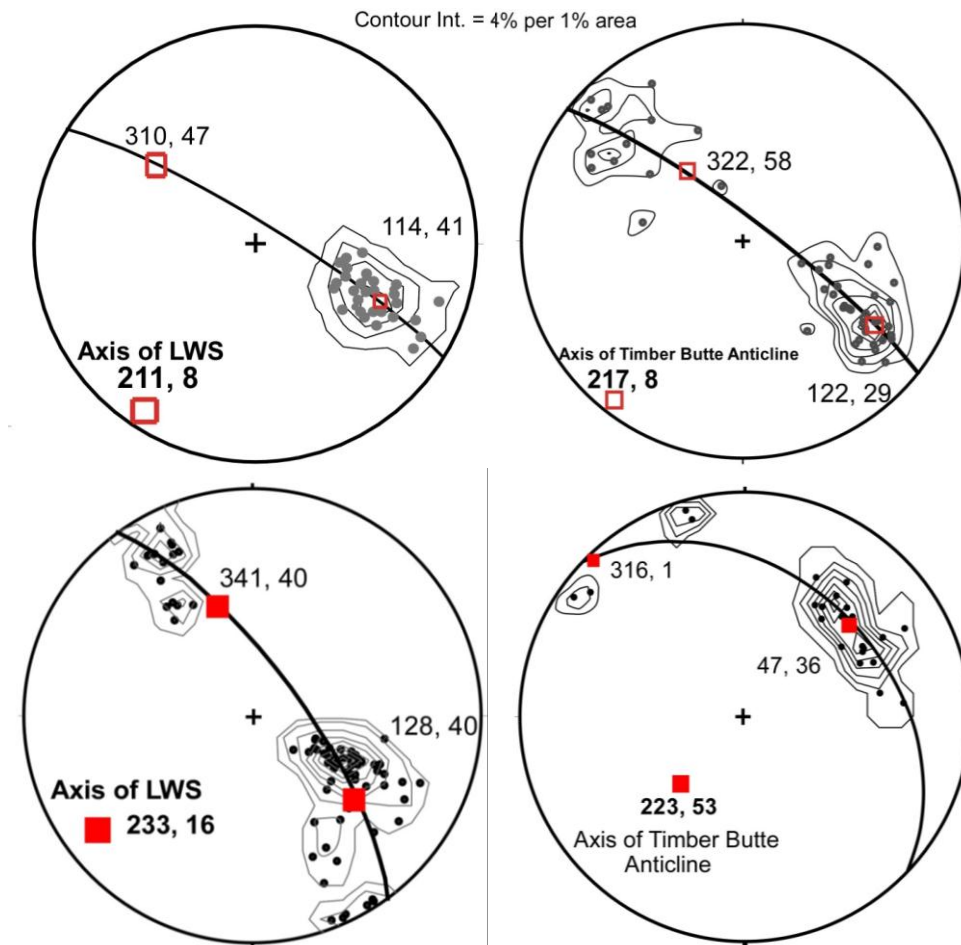


*Figure 10:* Stereonets of compiled attitudes (dots), created using STEREOWIN 1.2. Contour interval is 4% per 1 % area. These stereonet reveal the orientation of the Little Water syncline and the Timber Butte anticline.

*Upper left:* the average orientation (Trend and Plunge:  $211^{\circ}$ ,  $8^{\circ}$ SW) of the upright bedding of the Thaynes Formation, Mouth of LWS.

*Bottom Left:* attitudes from the Kootenai Formation of the Little Water syncline show a trend of  $233^{\circ}$ ,  $16^{\circ}$  SW.

*Top Right:* Attitudes from Thaynes and Dinwoody Formations of the Timber Butte anticline show a trend of  $217^{\circ}$ ,  $8^{\circ}$  SW.

*Bottom Right:* Attitudes from the Jurassic Strata and Beaverhead Formation show a trend of  $223^{\circ}$ ,  $53^{\circ}$  SW.

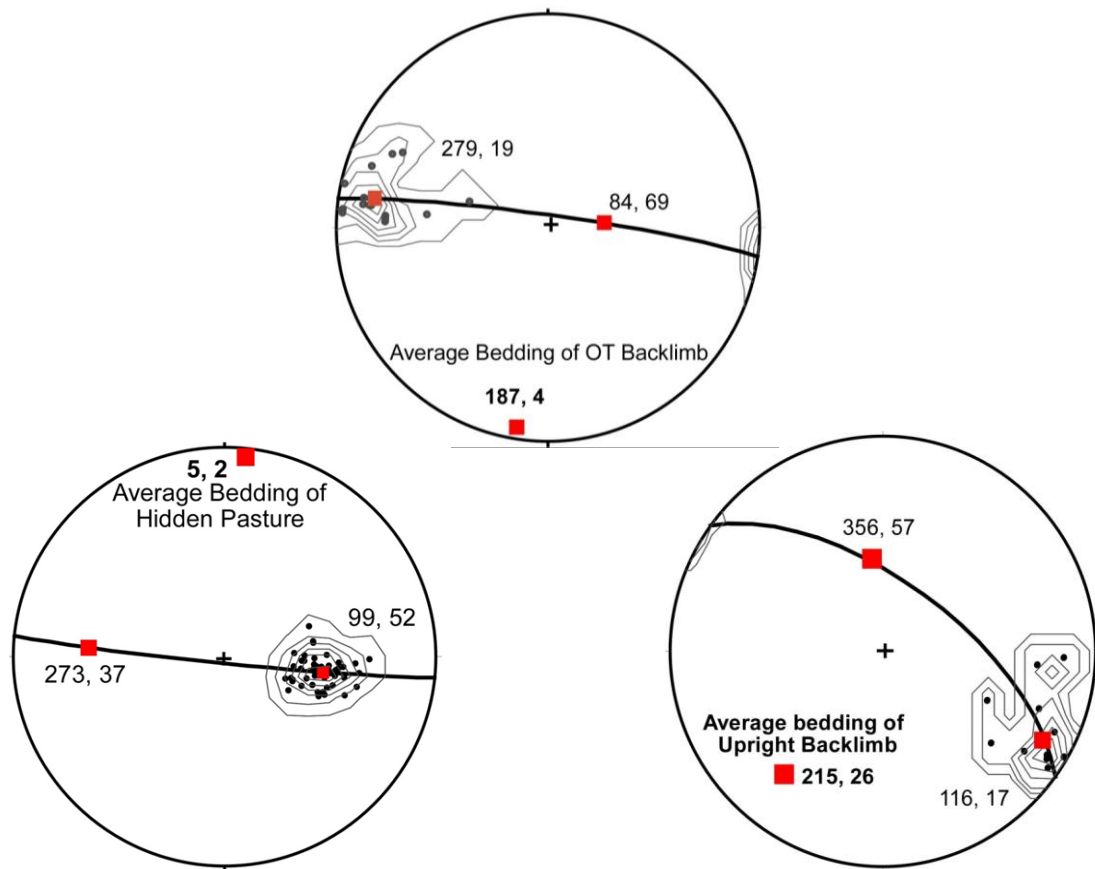


*Figure 11:* Stereonets of compiled attitudes (dots) of bedding surfaces in Hidden Pasture Canyon and the overturned and upright southwestern exposures of the Thaynes Formation.

*Left:* Attitudes taken in Hidden Pasture Canyon reveal an average orientation of bedding trending  $5^{\circ}$ , plunging  $2^{\circ}$ N.

*Center:* The average bedding of the southwestern overturned backlimb of the Thaynes Formation, trend and plunge:  $187^{\circ}$ ,  $4^{\circ}$ S.

*Right:* The average bedding of the upright southwestern exposure of the Thaynes Formation, trend and plunge:  $215^{\circ}$ ,  $26^{\circ}$ SW

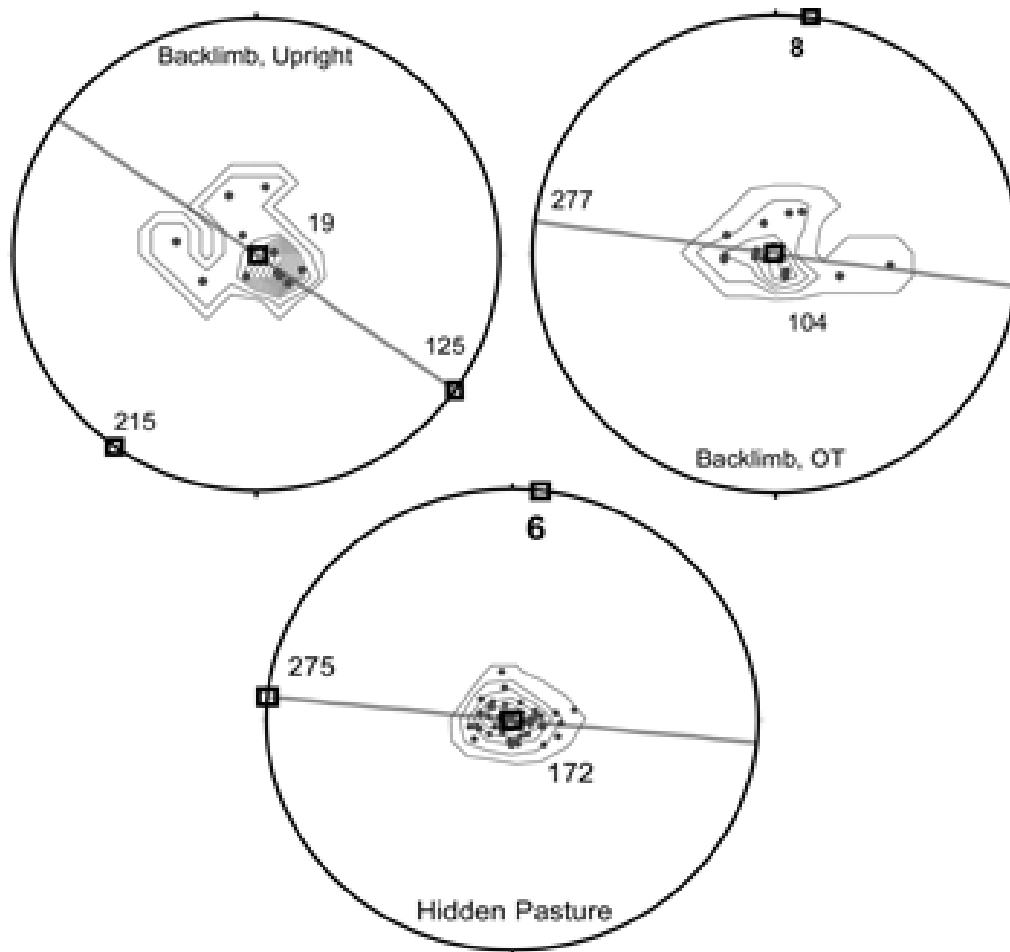


*Figure 12: Stereonets restored to horizontal and corrected for trend and plunge show original orientation of bedding surfaces. Contour interval is 4% per 1% area.*

*Top Right and Left: Retro-deformation of the southwestern exposure of the Thaynes Formation.*

*Bottom: Retro-deformation of Thaynes Formation bedding in Hidden Pasture Canyon.*

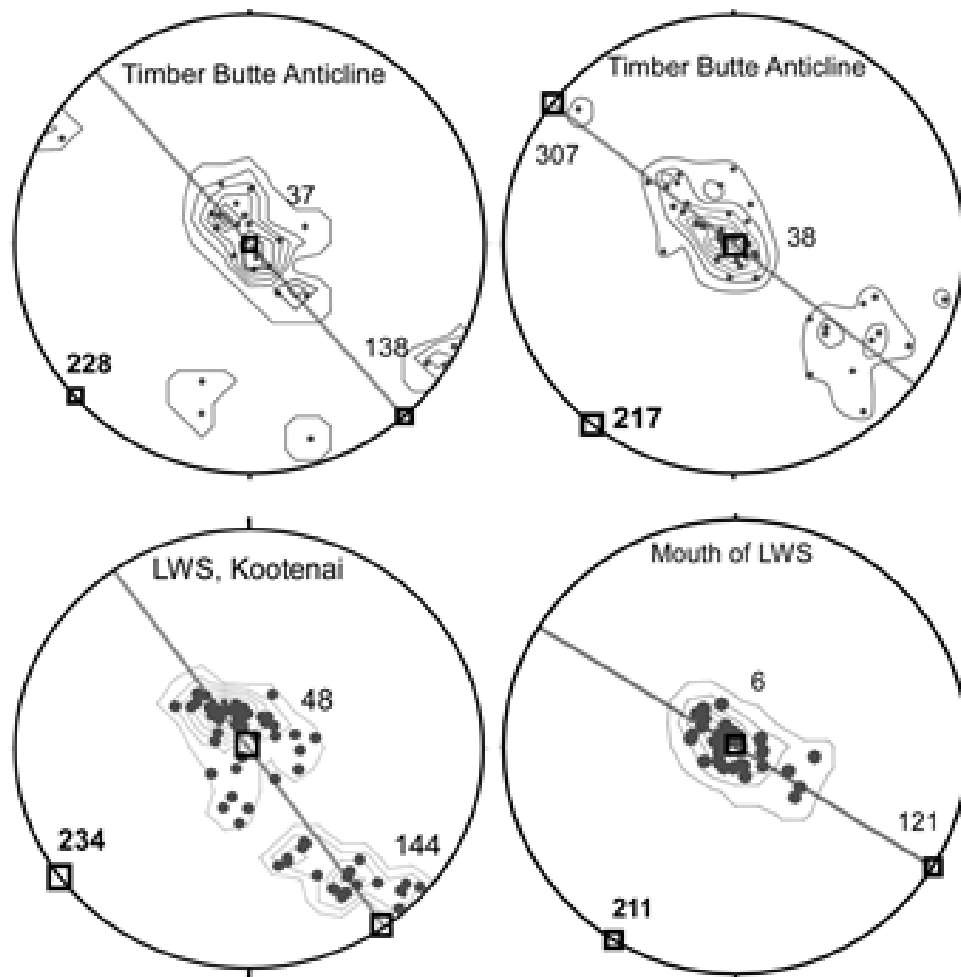


*Figure 13:* Stereonets restored to horizontal and corrected for trend and plunge show the bedding of the Thaynes formation prior to deformation. Contour interval is 4% per 1% area.

*Top Left and Right:* Retro-deformation of the Thaynes Formation on the Timber Butte anticline.

*Bottom Left and Right:* Retro-deformation of Thaynes Formation in the Little Water syncline.

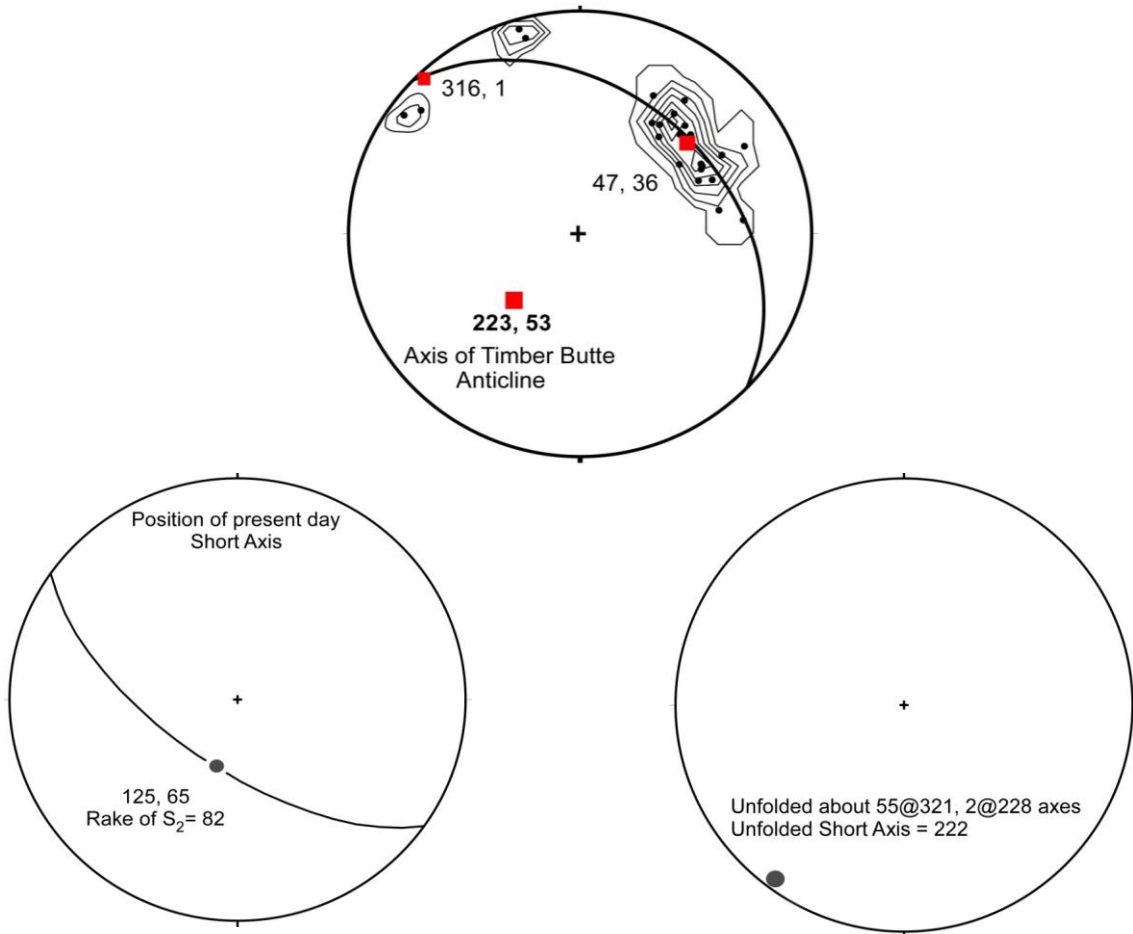


*Figure 14:* An example of the steps taken to uncover the initial LPS strain orientation.

*Top:* Stereonet showing axis of Timber Butte anticline, the location of sample LWS-PC-4a.

*Bottom Left:* Short axis of ellipse plotted on bedding of sample LWS-PC-4a.

*Bottom Right:* Retro-deformed (based on retro-deformations of the axis of the Timber Butte anticline) short axis of strain ellipse and bedding of LWS-PC-4a reveals a short axis orientation and initial LPS strain at  $222^\circ$ .



Table 2: Axes of rotation for performing retro-deformation of beddings surfaces containing strain ellipses.

<b>NETS</b>	<b>1stAOR</b>	<b>Rotamt1</b>	<b>2ndAOR</b>	<b>Rotamt2</b>	<b>NumPts</b>
<b>BcklmbUP</b>	<b>279.5</b>	<b>4.8°</b>	<b>187.8</b>	<b>70.6°/36°</b>	<b>12</b>
<b>BcklmbOT</b>	<b>296.5</b>	<b>26.8°</b>	<b>214.8</b>	<b>-74.2°/36°</b>	<b>16</b>
<b>HP</b>	<b>273.7</b>	<b>-2.6°</b>	<b>5.7</b>	<b>37.7°/36°</b>	<b>54</b>
<b>TBA1(tight)</b>	<b>316.2</b>	<b>55°</b>	<b>228.9</b>	<b>-2°</b>	<b>27</b>
<b>TBA2(broad)</b>	<b>322.5</b>	<b>8.6°</b>	<b>217</b>	<b>-57.7°</b>	<b>48</b>
<b>LWSbasin</b>	<b>341.2</b>	<b>17.5°</b>	<b>234.5</b>	<b>-42.3°</b>	<b>75</b>
<b>LWSmouth</b>	<b>310.6</b>	<b>8.1°</b>	<b>211.8</b>	<b>133.1°</b>	<b>38</b>

**NETS:** Correspond with Figures 10 and 11 stereonet. *BcklmbUP*, *BcklmbOT*: portions of the Thaynes Formation of Muddy Creek basin are overturned; *HP*: rotations performed on bedding in the Hidden Pasture area; *TBA1(tight)*: rotations performed on the tightened, de-coupled nose of the Timber Butte anticline; *TBA(broad)*: rotations performed on bedding on the rest of the Timber Butte anticline; *LWSbasin*: rotations performed on bedding in the Kootenai and Blackleaf Formations of the Little Water syncline; *LWSmouth*: rotations performed at the mouth of the Little Water syncline, near the Red Rock Fault.

**1stAOR:** Orientation of first axis of retro-deformation.

**Rotamt1:** Degrees of retro-deformation along the first axis of rotation.

**2ndAOR:** Orientation of second axis of retro-deformation.

**Rotamt2:** Degrees of retro-deformation along second axis of rotation.

**NumPts:** Number of points rotated.

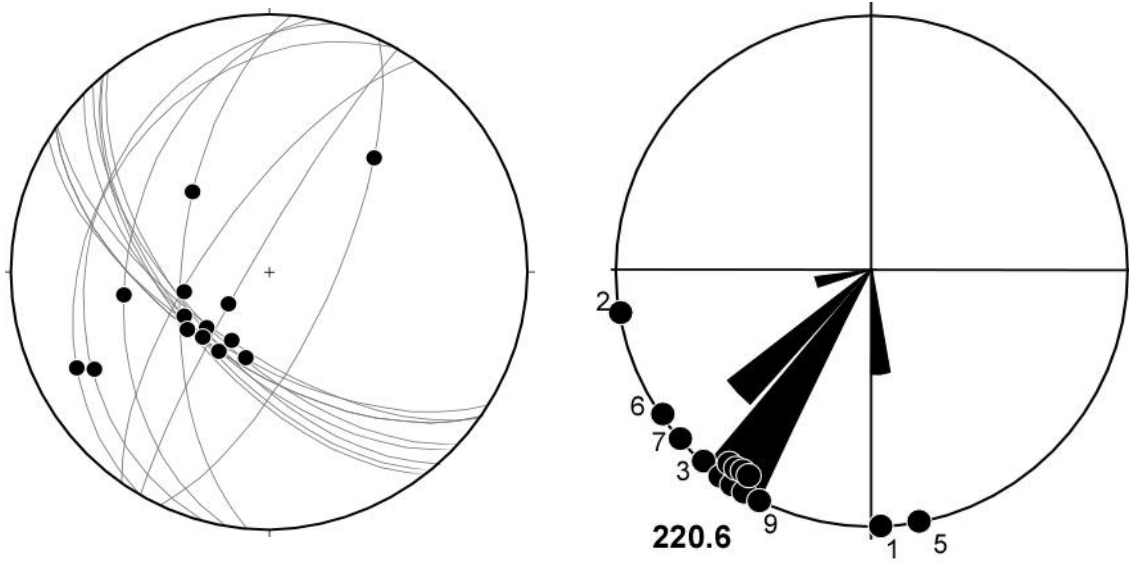


*Figure 15:* Stereonet and rose diagram illustrating the outcome of retro-deformation of collected sample strain ellipses.

*Left:* The orientation of the short axes of all strain ellipses used in this study, prior to retro-deformation.

*Right:* After retro-deformation, the short axes of nearly all ellipses cluster in the southwest quadrant of the rose diagram, yielding an average shortening direction of 220.6°.

## RESULTS AND DISCUSSION

When bedding is unfolded, LPS-strain indicators in bedding of the Thaynes Formation are oriented as such: 11 sites (3, 4, 6, 7, 8-14) are oriented  $\sim 221^\circ \pm 20^\circ$ ; 2 sites (1 and 5) are oriented  $\sim 175^\circ \pm 10^\circ$ ; and 1 site (2) at  $\sim 260^\circ$ . The LPS strain at 10 sites is consistent with NE-SW-shortening ( $\sim 221^\circ$ ) associated with the Sevier orogeny; the strain at 2 sites is consistent with N-S-shortening; and that at 1 site is consistent with E-W-shortening. Because no sites have LPS strain consistent with NW-SE-shortening, these results indicate that Sevier LPS strain occurred before Laramide deformation. The three sites where LPS strain lies outside of Sevier-shortening ( $221^\circ \pm 20^\circ$ ), but not within the

range of Laramide shortening ( $\sim 145^\circ \pm 10^\circ$ ) likely represent Sevier LPS strain affected by local factors not accounted for in the retro-deformational sequence used to restore bedding to horizontal in this study (small rotations, microfractures, etc.).

In previous studies, different conclusions were drawn; Perry et al. (1989) suggested that the Little Water syncline formed prior to thrusting of the Tendoy thrust system and was therefore moved NE and emplaced by later Sevier-style thrusting against a “Laramide buttress”. Their hypothesis was based upon a small number of oolitic samples containing calcite twins, stratigraphic correlation, and the presence of large, out-of-sequence segments of Beaverhead conglomerate which contain clasts that suggested erosion of the units from the Four Eyes Canyon thrust sheet, followed by propagation of the Sevier thrusts, followed by the Tendoy sheet over riding the Beaverhead conglomerates.

The strain ellipses determined in this study produce an interesting and complicated story of deformation in the research area. Ellipses 2, 3, 4, and 5 in the detached, western limb (Figure 16) show an intermediate amount of strain (out of all samples with ellipses) with compression associated with Sevier-style deformation. Preservation of this intermediate amount of shortening (Table 1, column %SH) is attributed to rapid overturning of these beds in the footwall syncline of the Four Eyes Canyon thrust. This bedding was apparently subjected to LPS strain only while horizontal; once it was rotated to a steep angle, the original LPS strain ellipses were preserved, and therefore were not subjected to further shortening. The sites 8-14 (Figure 16) show higher amounts of shortening (Table 1). In this case, this area was subjected to a longer period of Sevier-style LPS strain and/or greater strain rate before its bedding was rapidly folded about the NE-trending Laramide fold axes.

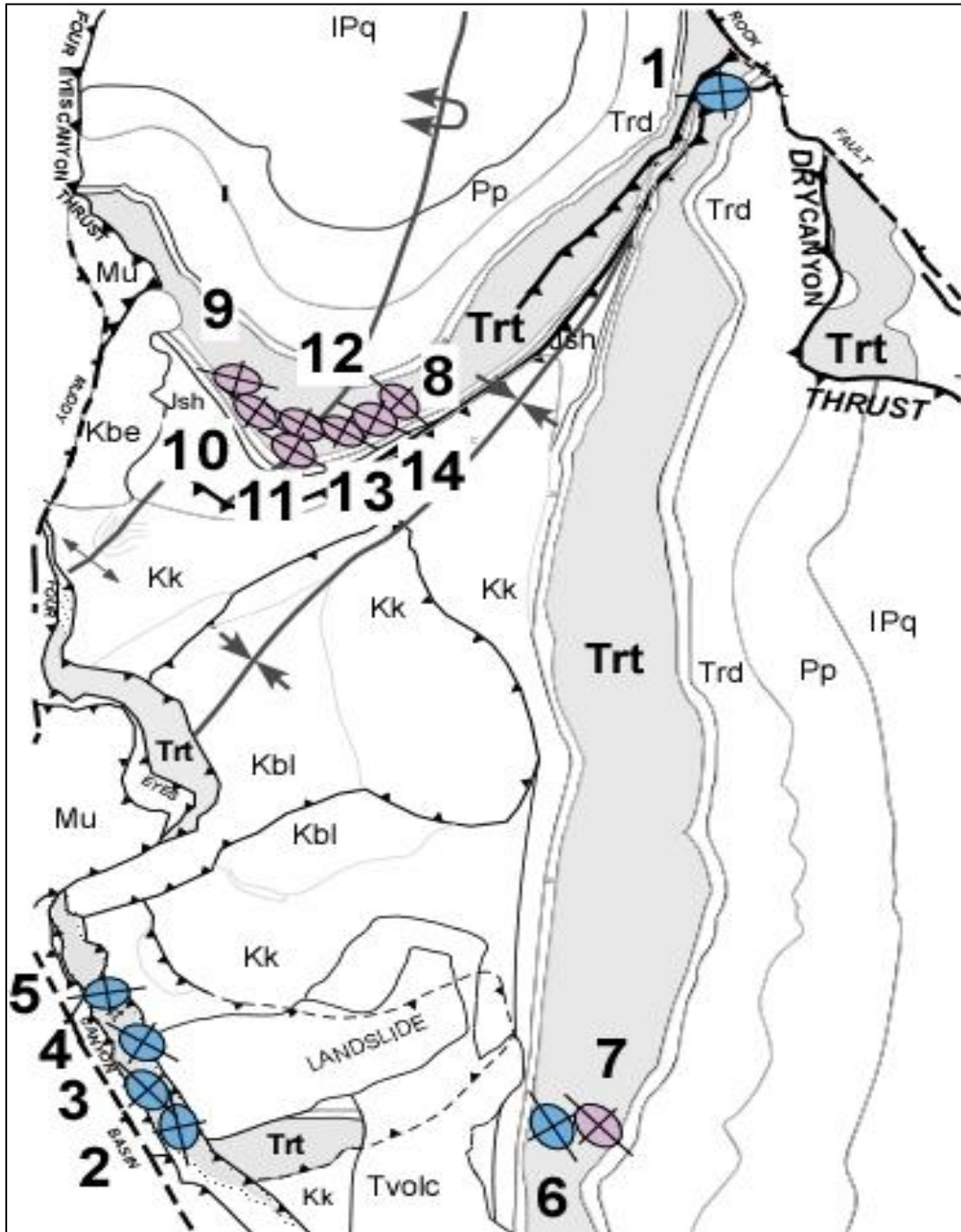


Figure 16: Strain ellipses. Sample numbers are derived from data displayed on Table 1.

As in the case of the Appalachian Roanoke recess (Whitaker & Bartholomew, 1999; Bartholomew & Whitaker, 2010), the LPS strain reflects strong early deformation.

### **CONCLUSION**

Upon sequentially retro-deforming the various bedding surfaces within the Thaynes Formation of the Timber Butte anticline, the Little Water syncline, Hidden Pasture Canyon and the western overturned backlimb of the syncline, LPS strain at 11 sites is consistent with the NE-SW-shortening ( $\sim 221^\circ$ ) associated with the Sevier orogeny; at 2 sites the LPS strain is consistent with N-S-shortening; and at 1 site is consistent with E-W-shortening. No sites have LPS strain consistent with NW-SE-shortening, and hence, we are left to conclude that Sevier LPS strain occurred before Laramide deformation in the research area.

This study is continuing, with more photographs collected for additional LPS-strain analysis, as well as collection of oolitic samples from another unit for total strain analysis. Mapping of the area also continues; all of these efforts will combine to provide a more comprehensive view of the sequence of deformation in the Little Water syncline part of the Tendoy thrust sheet.

## REFERENCES

- Aschoff, J. L. & Schmitt, J. G., 2004. Geologic map of the Dell 7.5-minute quadrangle, Cordilleran fold and thrust belt, Southwest Montana: Montana Bureau of Mines and Geology Open File Report, MBMG 520, 1:24,000-scale map, 33 p.
- Bally, A. W., Gordy, P. L., & Stewart, G. A., 1966. Structure, seismic data, and orogenic evolution of southern Canadian Rockies: *Canadian Society of Petroleum Geologists Bulletin* 14, p. 337-381.
- Bartholomew, M. J., 1989a. Structural relationship of the Little Water Syncline and thrusts of the Tendoy thrust system, southwestern Montana: *Geological Society of America, Abstracts with Programs* 21, No.5, p.54.
- Bartholomew, M. J., 1989b. Road Log no. 2: The Red Rock fault and complexly deformed structures in the Tendoy and Four Eyes canyon thrust sheets – Examples of Late Cenozoic and Late Mesozoic deformation in southwestern Montana: *Northwest Geology* 18, p. 21-35.
- Bartholomew, M. J., and Whitaker, A. E., 2010. The Alleghanian deformational sequence at the foreland junction of the central and southern Appalachians, in Tollo, R. P., Bartholomew, M. J., Hibbard, J. P., Karabinas, P. M., editors, 2010, ***From Rodinia to Pangea: The Lithotectonic Record of the Appalachian Region***: Boulder, Colorado, Geological Society of America Memoir 206, p. 431-454.
- Bartholomew, M. J., Greenwell, R. A., Wasklewicz, T. A., and Stickney, M. C., 2009. Alluvial fans: Sensitive tectonic indicators of fault-segmentation and tectonic regime partitioning along the Red Rock fault, southwestern Montana, USA: *Northwest Geology* 38, p. 41-66.
- Boyer, S. E., and Elliott, D., 1982. Thrust systems: *The American Association of Petroleum Geologists Bulletin* 66, no. 9, p. 1196-1230.
- Boyer, S. E., 1986. Styles of folding within thrust sheets: examples from the Appalachian and Rocky Mountains, U.S.A. and Canada: *Journal of Structural Geology* 8, nos. 3 and 4, p. 325-339.

- Couzens, B. A., Dunne, W. M., Onasch, C. M., and Glass, R., 1993. Strain variations and three-dimensional strain factorization at the transition from the southern to the central Appalachians: *Journal of Structural Geology* 15, p. 451-464.
- Crespi, J. M., 1986. Some guidelines for the practical applications of Fry's method of strain analysis: *Journal of Structural Geology* 8, p.799-808.
- De la Tour-du-Pin, H., 1983. Contribution a l'etude geologique de l'Overthrust Belt du Montana (USA); Stratigraphie at Tectonique des et du Hills et du Tendoy Range (Sud-Ouest Montana): Brest, France, Ph.D dissertation, Universitie de Bretagne Occidentale, 256 p.
- Dickinson W. R., 1988. Paleogeographic and paleotectonic setting of Laramide sedimentary basins in the Central Rocky Mountain region: *Geological Society of America, Bulletin* 100, p. 1023-1039.
- Dixon, J. S., 1982. Regional structural synthesis, Wyoming salient of western overthrust belt: *The American Association of Petroleum Geologists Bulletin* 66, no. 10, p. 1560-1580.
- Dunne, W. M., Onasch, C. M. & Williams, R. T.,1990. The problem of strain-marker centers and the Fry method: *Journal of Structural Geology* 12, p. 933-938.
- Dunlap, D. G., 1982. Tertiary geology of the Muddy Creek basin, Beaverhead County, Montana: Missoula, Montana, M.S. thesis, University of Montana, 133 p.
- Dyman, T. S., 1985a. Measured stratigraphic sections of Lower Cretaceous Blackleaf Formation and Lower upper Cretaceous Frontier Formation (Lower part) in Beaverhead and Madison counties, Montana: *US Geological Survey, Open-file Report*, p. 85-431.
- Dyman, T. S., 1985b. Stratigraphic and Petrologic analysis of Lower Cretaceous Blackleaf Formation and the Upper Cretaceous Frontier Formation (lower part), Beaverhead and Madison counties, Montana: Pullman, Washington, Ph.D. dissertation, Washington State University, 230 p.

- Dyman, T. S., Niblack, R., and Platt, J. E., 1984. Measured stratigraphic section of Lower Cretaceous Blackleaf Formation and Lower Upper Cretaceous Frontier Formation (lower part) near Lima, in southwest Montana: U. S. Geological Survey Open-file Report, 84-838, 25 p.
- Dyman, T. S., and Nichols, D. J., 1988. Stratigraphy of mid-Cretaceous Blackleaf and lower part of the Frontier Formation in parts of Beaverhead and Madison counties, Montana: *U.S. Geological Survey Bulletin* 1773, 31p.
- Dyman, T. S., Tysdal, R. G., Wallace, C. A., and Lewis, S. E., 1994. Correlation chart of Lower and Upper Cretaceous Blackleaf Formation, eastern Pioneer Mountains, southwestern Montana, to Drummond, central-western Montana: U.S. geological Survey, Miscellaneous Investigations Series, Map I-2478, 15 p., and 2 sheets.
- Dyman, T. S., Haley, J.C., and Perry, W. J., Jr., 1995. Conglomerate facies and contact relationships of the Upper Cretaceous upper part of the Frontier Formation and lower part of the Beaverhead Group, Lima Peaks area, southwestern Montana and southeastern Idaho, in *Shorter Contributions to the Stratigraphy and Geochronology of Upper Cretaceous Rocks in the Western Interior of the United States: U. S. Geological Survey Bulletin* 2113A, p. A1-A10.
- Dyman, T. S., Tysdal, R. G., and Perry, W. J., Jr., 1997. Correlation of Upper Cretaceous strata from Lima Peaks area to Madison Range, southwestern Montana and southeastern Idaho: *Cretaceous Research* 18, p. 751-766.
- Evans, M. A., & Dunne, W. M., 1991. Strain factorization and partitioning in the North Mountain thrust sheet, central Appalachians, USA: *Journal of Structural Geology* 13, p. 21-35.
- Erslev, E. A., Ge, H., 1990. Least-squares center-to-center and mean-object ellipse fabric analysis: *Journal of Structural Geology* 12, p. 155-162
- Fritz, W. J. & Sears J. W., 1993. Tectonics of the Yellowstone hotspot wake in southwestern Montana: *Geology* 21, p. 427-430.
- Fry, N., 1979. Random point distributions and strain measurement in rocks: *Tectonophysics* 60, p. 89-105.



- Gealy, W. J., 1953. Geology of the Antone Peak quadrangle, southwest Montana: Cambridge, Massachusetts, Ph.D. dissertation, Harvard University, 115 p.
- Genier, F., & Epard, J., 2006. The Fry method applied to an augen orthogneiss: Problems and results: *Journal of Structural Geology* 29, p. 209-224.
- Gwinn, V. E., 1965. Cretaceous rocks of the Clark Fork valley, central/western Montana: Billings, Montana, Billings Geological Society 16th Annual Guidebook, p. 34-57.
- Haley, J. C., 1983a. Depositional processes in Beaverhead Formation, southwestern Montana and northeastern Idaho: *Geological Society of America Abstracts with Programs* 16, no. 6, p. 589.
- Haley, J. C., 1983b. The sedimentology of a synorogenic deposit; The Beaverhead Formation of Montana and Idaho: *American Association of Petroleum Geologists Bulletin* 67, p. 1340
- Haley, J. C., 1986. Upper Cretaceous (synorogenic) deposits of the Montana-Idaho thrust belt and adjacent foreland: Relationships between sedimentation and tectonism: Baltimore, Maryland, Ph.D. Dissertation, Johns Hopkins University, 542 p.
- Haley, J. C., and Perry, W. J., Jr., 1991. The Red Butte Conglomerate - a thrust-belt-derived conglomerate of the Beaverhead Group, southwestern Montana: *U. S. Geological Survey Bulletin* 1945, 19p.
- Hammons, P. M., 1981. Structural observations along the southern trace of the Tendoy fault, southern Beaverhead County, Montana; in Tucker, T.E., ed., ***Southwest Montana: Montana Geological Society Field Conference and Symposium guidebook***: p. 253-260.
- Harkins, N. W., Latta, D. K., Anastasio, D. J., Pazzaglia, F. J., 2004. Surficial and bedrock geologic map of the Dixon Mountain 7.5' quadrangle, southwest Montana: Montana Bureau of Mines Open Field Report 495, 13 pgs.
- Janecke, S. U., 1994. Sedimentation and paleogeography of an Eocene to Oligocene rift zone, Idaho and Montana: *Geological Society of America Bulletin* 106, p. 1083-1095.

- Janecke, S. U., McIntosh, W., Good, S., 1999. Testing models of rift basins: structure and stratigraphy of an Eocene-Oligocene supra-detachment basin, Muddy Creek half graben, southwestern Montana: *Basin Research* 2, p. 143-167.
- Janecke, S. U., VanDenburg, C. J., Blankenau, J. J., 1998. Geometry, mechanisms, and significance of extensional folds from examples in the Rocky Mountain Basin and Range province, U.S.A.: *Journal of Structural Geology* 20, pp. 841-856.
- Janecke, S. U., Skipp, B., Perry, W. J., Jr., 2000. Revised thrust fault patterns in the Tendoy Mountains of southwestern Montana: *Geological Society of America Abstracts with Programs*, Rocky Mountain Section 32, no. 5, p. A-12.
- Janecke, S. U., VanDenberg, C. J., Blankenaw, J., M'Gonigle, J. W., 2000. Long distance longitudinal transport of gravel across the Cordilleran thrust of Montana and Idaho: *Geology* 28, p. 439-442.
- Johnson, P. P., 1981a. Geology of the Red Rock Fault and adjacent Red Rock valley, Beaverhead county, Montana: Missoula, Montana, M.S. thesis, University of Montana, 88 p.
- Johnson, P. P., 1981b. Geology along the Red Rock fault and adjacent Red Rock basin, Beaverhead county, Montana; *in* Tucker, T.E., ed., ***Southwest Montana: Montana Geological Society Field Conference and Symposium Guidebook***: p. 245-251.
- Keunzi, W. D., & Fields, R. W., 1971, Tertiary Stratigraphy, Structure, and Geologic History, Jefferson Basin, Montana: *Geological Society of America Bulletin* 82, no. 12, p. 3373-3394.
- Klecker, M. R., 1981. Lower Triassic strandline deposits near Dell, Montana; *in* Tucker, T.E., ed., ***Montana Geological Society Field Conference and Symposium Guidebook***: p. 71-81.
- Klecker, R. A., 1980. Stratigraphy and structure of the Dixon Mountain- Little Water Canyon area, Beaverhead County, Montana: Corvallis, Oregon, M. S. thesis, Oregon State University, 223 p.

- Klepper, M. R., 1950. A geologic reconnaissance of parts of Beaverhead and Madison counties, Montana: *U. S. Geological Survey Bulletin* 969-C, 85 p., 1 map, scale 1:250,000.
- Kulik, D. M., & Perry, W. J., 1988. The Blacktail-Snowcrest foreland uplift and its influence on the structure of the Cordilleran thrust belt- Geological and geophysical evidence for the overlap province in southwestern Montana, *in* Schmidt, C. J., and Perry, W. J., Jr., eds., ***Interaction of the Rocky Mountain Foreland and the Cordilleran Thrust Belt***: Geological Society of America Memoir 171, p. 291-306.
- Lonon, J. D., Skipp, B., Ruppel, E. T., Janecke, S. U., Perry, W. J., Jr., Sears, J. W., Bartholomew, M. J., Stickney, M. C., Fritz, W. J., Hurlow, H. A., and Thomas, R. C., 2000. Geologic Map of the Lima 30' x 60' quadrangle southwest Montana: Montana Bureau of Mines and Geology, Open File 408, 1:100,000-scale map plus text.
- Majerowicz, C. N., Anderson, L. D., Anastasio, D. J., and Pazzaglia, F. J., 2007. Bedrock and Surficial Geologic Map of the Henry Gulch 7.5' Quadrangle Beaverhead County, Southwest Montana: Montana Bureau of Mines and Geology, Open File Report 563, 19p. 1sheet, scale 1:24,000.
- McKelvey, V. E., Williams, J. S., Sheldon, R. P., Cressman, E. R., Cheney, T. N., and Swanson, R. W., 1956. The Phosphoria, Park City, and Shedhorn Formations in the western phosphate field: advanced summary: *American Association of Petroleum Geologists Bulletin* 40, p. 2826-2863.
- McDowell, R. J., 1997. Evidence for synchronous thin-skinned and basement deformation in the Cordilleran fold and thrust belt, the Tendoy Mountains, southwestern Montana: *Journal of Structural Geology* 19, p.77-87.
- McDowell, R. J., 1998. Along-strike variations in structural geometry of thrust sheets in the Tendoy Mountains, southwestern Montana: *The Mountain Geologist* 35, no. 1, p. 31-40.
- Moritz, C. A., 1951. Triassic and Jurassic stratigraphy of southwestern Montana: *American Association of Petroleum Geologists Bulletin* 35, p. 1781-1814.

- Nichols, D. J., Perry, W. J., Haley, J. C., 1985. Reinterpretation of palynology and age of Laramide syntectonic deposits, southwestern Montana, Revision of Beaverhead Group: *Geology* 13, p. 149-153.
- Oldow, J. S., Bally, A. W., Leeman, W. P., 1989. Phanerozoic evolution of the North American Cordillera, United States and Canada, *in* Bally, A. W., and Palmer, A. R., eds., *The Geology of North America — An Overview, The Geology of North America, Vol. A*: Boulder, Colorado, Geological Society of America, p. 139–232.
- Onasch, C. M., & Dunne, W. M., 1992. Variation in quartz arenite deformation mechanisms between a roof sequence and duplexes: *Journal of Structural Geology* 14, p. 24-36.
- Pecora, W. C., 1981. Bedrock geology of the Blacktail Mountains, southwestern Montana [M.S. thesis]: Middletown, Connecticut, Wesleyan University, 203 p.
- Perry, W. J., Jr., 1986. Critical deep drillholes and indicated Paleozoic paleotectonic features north of the Snake River downward in southern Beaverhead County, Montana and adjacent Idaho: U.S. Geological Survey Open-File Report 86-413, 16p.
- Perry, W. J., & Sando, W. J., 1982. Sequence of deformation of Cordilleran thrust belt in Lima, Montana region, *in* Powers, R. B., ed., *Geologic Studies of the Cordilleran Thrust Belt*: Denver, Colorado, Rocky Mountain Association of Geologists 1, p. 137-144.
- Perry, W. J., Ryder, R. T., Maughan, E. K., 1981. The southern part of the southwest Montana thrust belt, *in* Tucker, T. E., ed., *Southwest Montana: Montana Geological Society Field Conference 1981 Guidebook*: p. 261-273.
- Perry, W. J., Wardlaw, B. R., Bostick, N. H., Maughan, E. K., 1983a. Structure, burial history and petroleum potential of frontal thrust belt and adjacent foreland, southwest Montana: *American Association of Petroleum Geologists Bulletin* 67, no. 5, p. 727-743.
- Perry, W. J., Rice, D. D., Maughan, E. K., 1983b. Petroleum potential of wilderness lands in Montana: Washington, D.C., U. S. Geological Survey Circular 902-G, 23 p.

- Perry, W. J., Hossack, J. R., 1984. Structure of the frontal zone, southwest Montana sector of the Cordilleran thrust belt: Geological Society of America, Abstracts with programs 16, no.6, p.622.
- Perry, W.J., Sando, W.J., Sandberg., C.A., 1985. Structural geometry of newly defined Blacktail salient of Montana thrust belt [abs]: *AAPG Bulletin* 69, no.5, p. 858-859.
- Perry, W. J ., Haley, J. C., Nichols, D. J., Hammons, P. M., 1988. Interactions of Rocky Mountain foreland and Cordilleran thrust belt in Lima region, southwest Montana, in Schmidt, C.J., and Perry, W. J., Jr., eds., ***Interaction of the Rocky Mountain Foreland and the Cordilleran Thrust Belt***: Boulder, Colorado, Geological Society of America Memoir 171, p. 267-289.
- Perry, W. J. Jr., Dyman, T. S., Sando, W. J., 1989. Southwestern Montana recess of the Cordilleran thrust belt, in French, D. E., and Grabb, R. F., eds., ***Geologic Resources of Montana***: Montana Geologic Society, 1989 Field Conference Guidebook, p. 261-270.
- Perry, W. J., Jr., Dyman, T. S., Guthrie, G. E., 1989. Trip 2 Road Log - Tectonics and mid-Cretaceous rocks of southwest Montana recess of Cordilleran thrust belt, in French, D. E., and Grabb, R. F, eds., ***Geologic Resources of Montana***: 1989 Field Conference Guidebook, Montana Geological Survey, p. 438-448.
- Perry, W. J., Jr., Dyman, T. S., Sando, W. J., 1989. Southwestern Montana recess of Cordilleran thrust belt, in French, D. E., and Grabb, R. F., eds., ***Geologic Resources of Montana***: 1989 Field Conference Guidebook, Montana Geological Survey, p. 261-270.
- Peterson, J. A., 1981. General stratigraphy and paleostructure of the western Montana overthrust belt, in Tucker, T. E., ed., ***Southwest Montana: Montana Geological Society Field Conference and Symposium Guidebook***, p. 5-35.
- Peterson, J. A., 1985. Regional stratigraphy and general petroleum geology of Montana and adjacent areas, in ***Montana Oil Fields Symposium, 1985***: Billings, Montana, Montana Geological Society, p. 5-45.
- Ponton, J. D., 1983. Structural analysis of the Little Water syncline, Beaverhead County, Montana: College Station, Texas, Texas A & M University, M.S. Thesis, 165 p.

- Ramsay, J.G., & Huber, M. I., 1983. The Strain Ellipse: Concept, Distortion and Rotation, in Ramsay, J.G., Huber, M. I., *The Techniques of Modern Structural Geology*: London, United Kingdom, Academic Press 1, 307 p.
- Ruppel, E. T., & Lopez, D. A., 1984. *The Thrust Belt in Southwest Montana and East-Central Idaho*: Washington, D.C., U.S. Geological Survey Professional Paper 1278, 41 p.
- Ryder, R. T., Ames, H. T., 1970. The palynology of the Beaverhead Formation and their paleotectonic implications in the Lima region, Montana-Idaho: *American Association of Petroleum Geologists Bulletin* 54, p.1155-1171.
- Ryder, R. T., & Scholten, R., 1973. Syntectonic conglomerates in southwest Montana: their nature, origin and tectonic significance: *Geological Society of America Bulletin*, v. 84, p. 773-796.
- Sadler, R. K., 1980. Structure and stratigraphy of the Little Sheep Creek area, Beaverhead County, Montana: Oregon State University M.S. Thesis, 294p.
- Sandberg, C. A., & Mapel, W. J., 1967. Devonian of the northern Rocky Mountains and Plains, in Oswald, D. H., ed., *International Symposium on the Devonian System*: Calgary, Alberta, September 1967: Calgary, Alberta, Alberta Society of Geologists 1, p. 843-877.
- Sandberg, C.A., Gutschick, R.C., Johnson, J.G., Poole, F.G., Sando, W.J., 1983. Middle Devonian to Late Mississippian history of the overthrust belt region, western United States, in Powers, ed., *Geologic Studies of the Cordilleran Thrust Belt, 1982*: Denver, CO, Rocky Mountain Association of Geologists 2, p. 691-719.
- Sando, W.J., Sandberg, C.A., Perry, W.J., 1985. Revision of Mississippian stratigraphy, northern Tendency Mountains, southwest Montana: USGS Bulletin 1656-A, p. A1-A10.
- Saperstone, H. I., & Etheridge, F. G., 1984. Origin and paleotectonic setting of the Pennsylvanian Quadrant sandstone, southwestern Montana: Wyoming Geological Association 35<sup>th</sup> Annual Field Conference Guidebook, p. 309-331.

- Saperstone, H. I., 1986. Description of measured sections of the Pennsylvanian Quadrant Sandstone, Beaverhead, Madison, and Park counties, southwestern Montana: U.S. Geological Survey Open-File Report 86-182, 68p.
- Scholten, R., 1957. Paleozoic evolution of the geosynclinal margin north of the Snake River Plain, Idaho-Montana: *Geological Society of America Bulletin* 68, p. 151-170.
- Scholten, R., & Ramspott, L. D., 1968. **Tectonic Mechanisms Indicated by Structural Framework of Central Beaverhead Range, Idaho-Montana**: Washington, D.C., U.S. Geological Survey Special Paper 104, 70p.
- Scholten, R. K., Keenmon, A., Kupsch, W. O., 1955. Geology of the Lima region, southwestern Montana and adjacent Idaho: *Geological Society of America Bulletin* 66, p. 345 -404.
- Sears, J. W., & Fritz, W. J., 1998, Cenozoic tilt domains in southwestern Montana: Interference among three generations of extensional fault systems, *in* Faulds, J. E., and Stewart, J. H., eds., ***Accommodation Zones and Transfer Zones: The Regional Segmentation of the Basin and Range Province***: Boulder, Colorado, Geological Society of America Special Paper 323, p. 241-249.
- Sears, J. W., Hurlow, H., Fritz, W. J., and Thomas, R. C., 1995. Late Cenozoic disruption of Miocene grabens on the shoulder of the Yellowstone hotspot track in southwest Montana: Field guide from Lima to Alder Montana, *in* Mogk, D. W., ed., ***Field Guide to Geological Excursions in Southwest Montana***, for Rocky Mountain section, Geological Society of America Annual Meeting, Bozeman, Montana, May 16-21, 1995: *Northwest Geology* 24, p. 201-219.
- Sears, J. W., 2007. Sequential doming and faulting along the margin of the Yellowstone hot spot track in SW Montana: parameters to test the plume hypothesis from Neogene Sixmile Creek formation: *Geological Society of America, Abstracts with Programs* 39, no. 6, p. 292.
- Skipp, B., 1988. Cordilleran thrust belt and faulted foreland in the Beaverhead Mountains, Idaho and Montana, *in*: Schmidt, C. J., and Perry, W. J., Jr., eds., ***Interaction of the Rocky Mountain Foreland and Cordilleran Thrust Belt***: Boulder, Colorado, Geological Society of America Memoir 171, p. 237-266.

- Skipp, B., & Janecke, S. U., 2004. Geologic map of the Montana part of the Dubois 30' x 60' quadrangle, Idaho and Montana: Montana Bureau of Mines and Geology, Open File Report MBMG 490, scale 1:100,000.
- Simon, R. I., & Gray, D. R., 1982. Interrelations of mesoscopic structures and strain across a small regional fold, Virginia Appalachians: *Journal of Structural Geology* 4, p. 271-289.
- Sloss, L. L., & Moritz, C. A., 1951. Paleozoic stratigraphy of southwestern Montana: *American Association of Petroleum Geologists Bulletin* 35, p. 2135-2169.
- Spraggins, S. A., & Dunne, W. M., 2002. Deformation history of the Roanoke recess, Appalachians, USA: *Journal of Structural Geology* 24, p. 411-433.
- Stickney, M.C., & Bartholomew, M. J., 1987. Seismicity and late Quaternary faulting of the Northern Basin and Range province, Montana and Idaho: *Bulletin of the Seismological Society of America* 77, p. 1602–1625.
- Tysdal, R. G., Dyman, T. S., Lewis, S. E., 1994. Geologic map of Cretaceous strata between Birch Creek and Brownes Creek, eastern flank of Pioneer Mountains, Beaverhead County, Montana: U.S. Geological Survey. Miscellaneous Investigations Series, Map I-2434, 1:24,000-scale map plus text.
- Waldron, J. W. F., & Wallace, K. D., 2007. Objective fitting of ellipses in the centre-to-centre (Fry) method of strain analysis: *Journal of Structural Geology* 29, p. 1430-1444.
- Wardlaw, B. R., & Pecora, W. C., 1985. New Mississippian-Pennsylvanian stratigraphic units in southwest Montana and adjacent Idaho: U.S. Geological Survey Bulletin 1656-B, p. B1- B9.
- Whitaker, A. E., & Bartholomew, M. J., 1999. Layer parallel shortening: a mechanism for determining deformation timing at the junction of the central and southern Appalachians: *American Journal of Science* 259, p. 238-254.
- Wilson, J. L., 1970. Depositional facies across carbonate shelf margins: *Transactions of Gulf Coast Association of Geologists Society* 20, p. 229-233.



Williams, N. S., 1984. Stratigraphy and structure of the east-central Tendoy Range, southwestern Montana: Chapel Hill, North Carolina, University of North Carolina M.S. Thesis, 94p.

Williams, N. S., & Bartley, J. M., 1988. Geometry and sequence of thrusting, McKnight and Kelmbeck Canyons, Tendoy Range, Southwestern Montana, *in* Schmidt, C.J., and Perry, W. J., Jr., eds., ***Interaction of the Rocky Mountain foreland and the Cordilleran thrust belt***: Boulder, Colorado, Geological Society of America Memoir 171, p. 307-318.

Wilson, M. D., 1970. Upper Cretaceous-Paleocene synorogenic conglomerates of southwestern Montana: *American Association of Petroleum Geologists Bulletin* 54, p. 1843-1867.